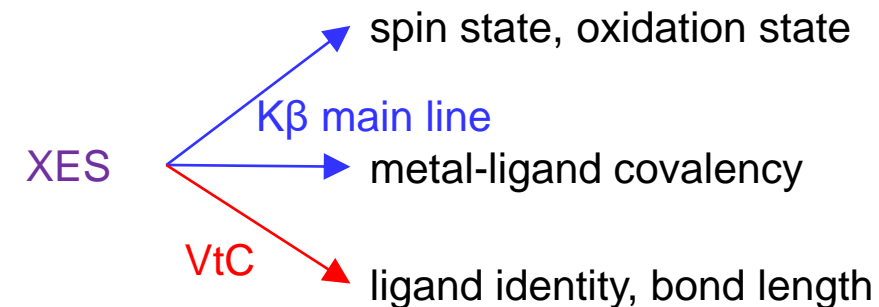
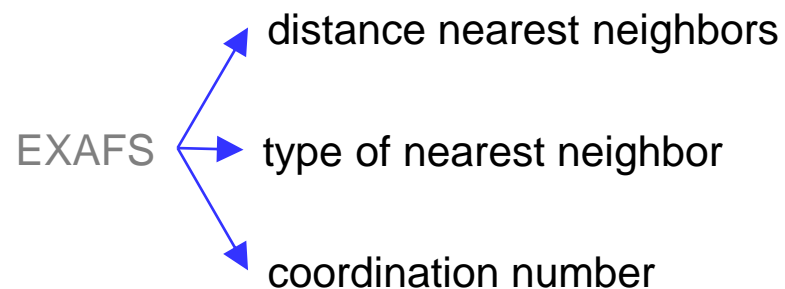
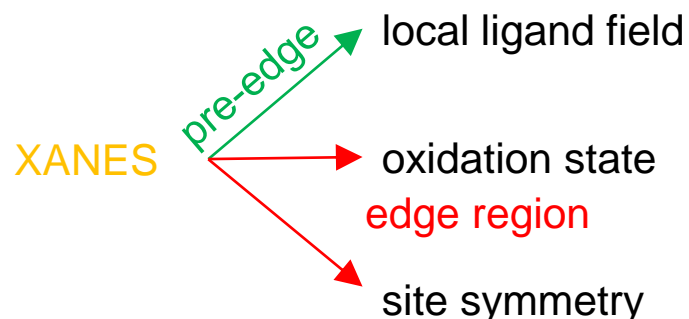
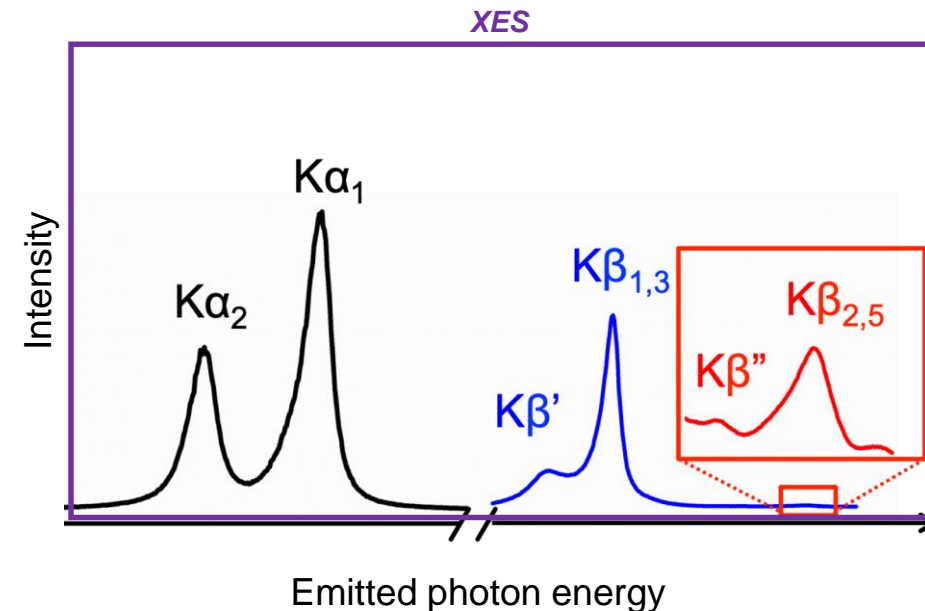
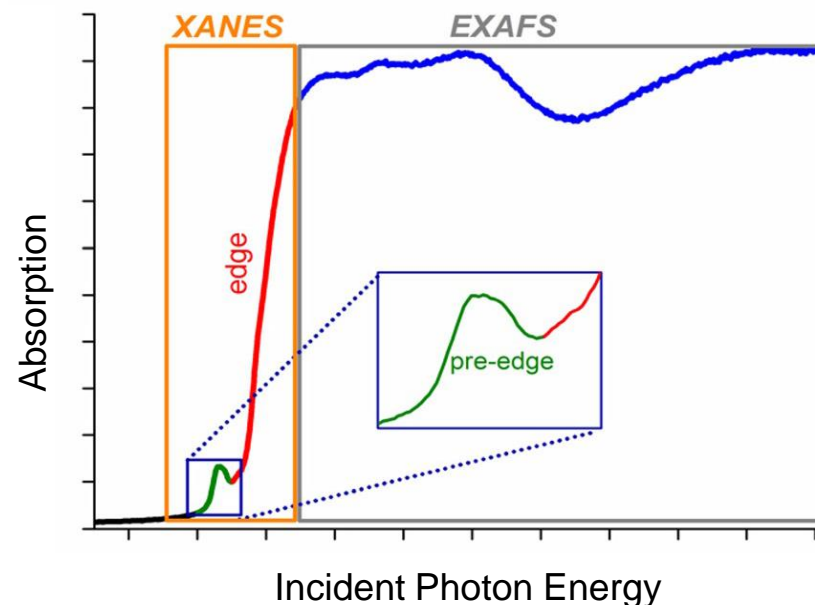
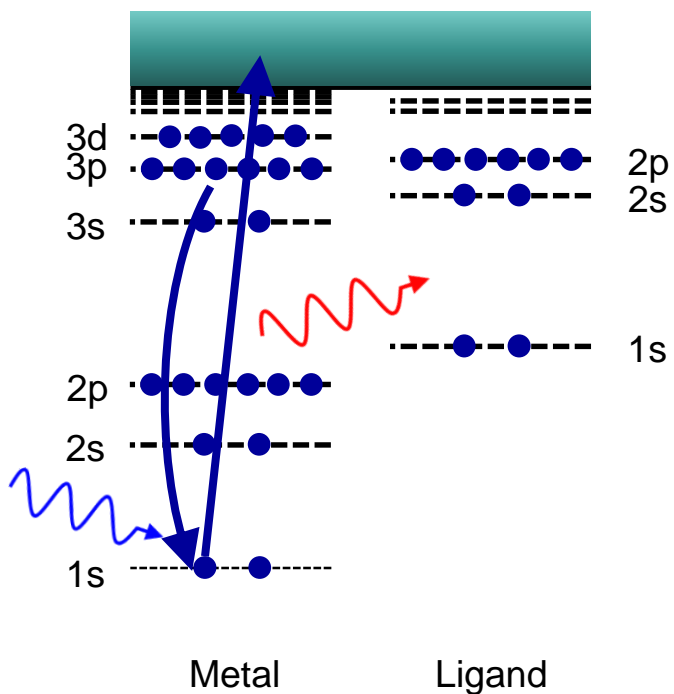


IN-HOUSE X-RAY SPECTROSCOPY AT THE MPI CEC UPDATE AND APPLICATIONS

Yves Kayser, Carl Camayang, Christian Feike, Philipp Manthey,
Diana Tiburcio, Serena DeBeer

Max Planck Institute for Chemical Energy Conversion
yves.kayser@cec.mpg.de

X-RAY ABSORPTION FINE STRUCTURE SPECTROSCOPY



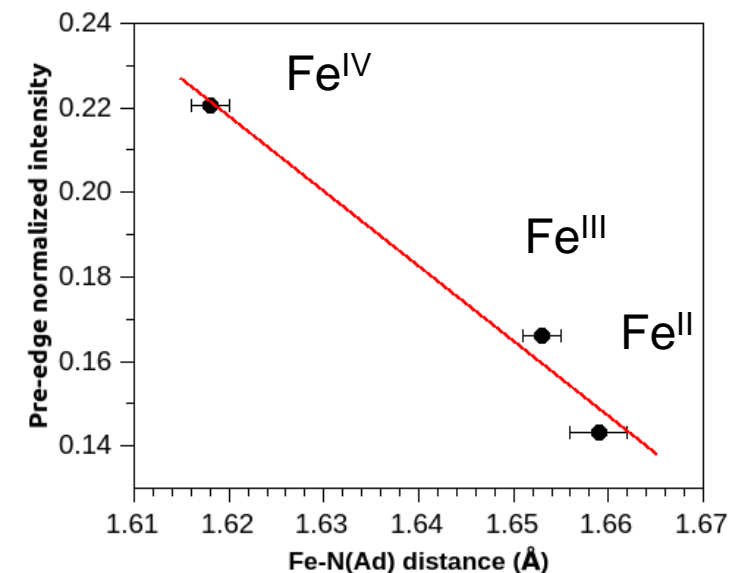
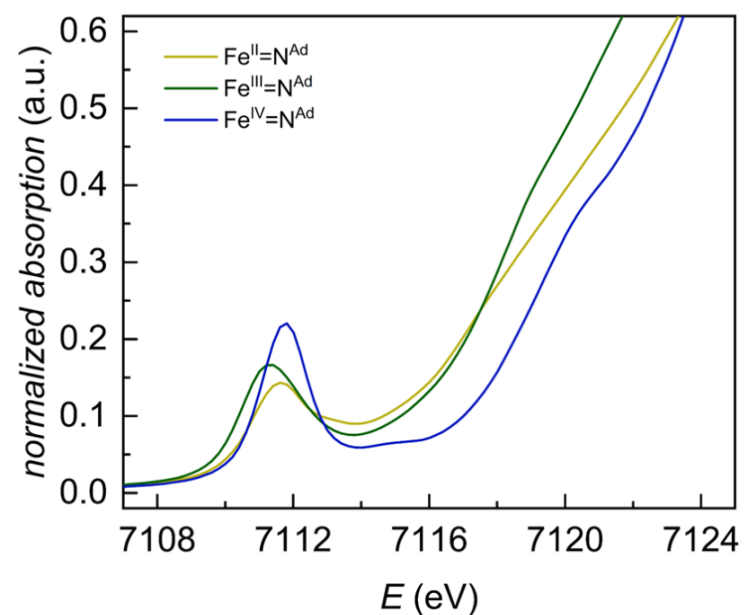
METAL-LIGAND BOND AND PRE-EDGE INTENSITY

Short, strong covalent bonds in non-centrosymmetric systems tend to increase pre-edge intensity

	Fe–N ^{Ad} (Å)	Calc. main pre-edge intensity*
Fe ^{II}	1.659(3)	1.08
Fe ^{III}	1.653(2)	2.64
Fe ^{IV}	1.618(2)	4.06

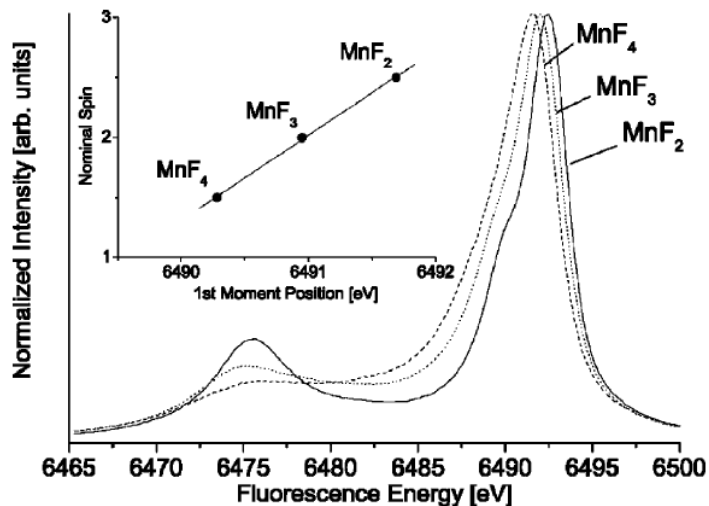
* most intense calculated transition in the pre-edge region

Experiment



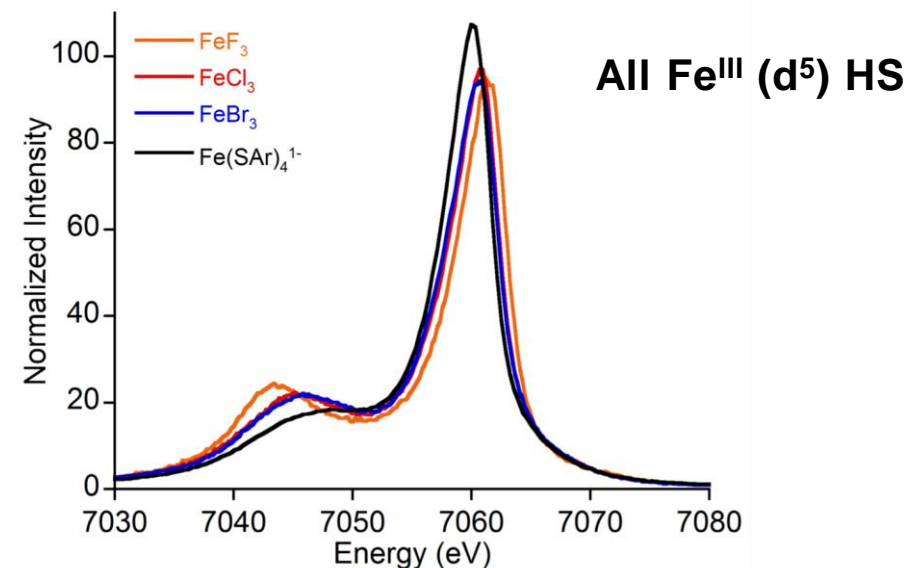
J. Am. Chem. Soc. 145, 2, 873-887 (2023).

XES: SPIN STATE AND COVALENCY



- $K\beta_{1,3}$ and $K\beta'$ move closer together with decreasing spin state (i.e. as 3p-3d exchange interaction decreases)
- $K\beta$ lines reflect number of unpaired d electrons
- Require very little time to measure (minute(s) using SR) or minutes to hours with a stand-alone source.

Coord. Chem. Rev. 249, 65 (2005).



- Even for a series of high spin ferric compounds, large variations in the $K\beta$ mainlines are observed
- Change in ΔE > of over 4.5 eV
- If nominal spin is known (by other methods) covalency can be extracted.
- Emphasizes importance of combined methods.

J. Am. Chem. Soc. 136, 9453 (2014).

IN-HOUSE X-RAY SPECTROSCOPY FACILITIES AT THE CEC

XES
XAS
EXAFS

Hard X-ray
radiation



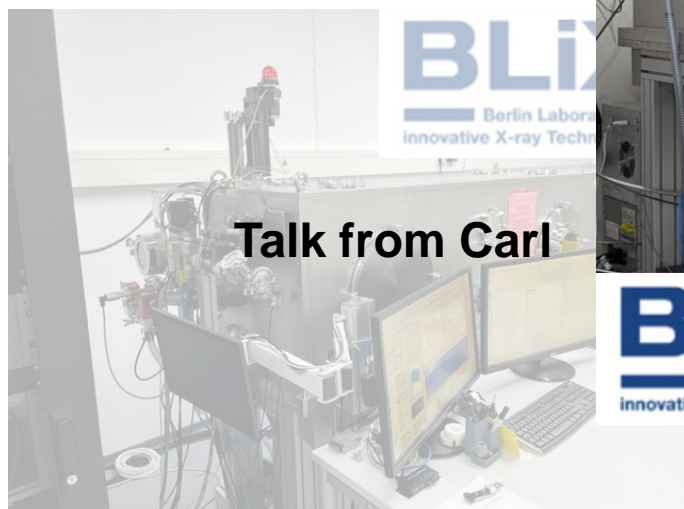
 easyXAFS



BLiX
Berlin Laboratory for
innovative X-ray Technologies

XES

Tender to
hard X-ray
radiation



Talk from Carl

BLiX
Berlin Laboratory for
innovative X-ray Technologies

EXAFS

Hard X-ray
radiation



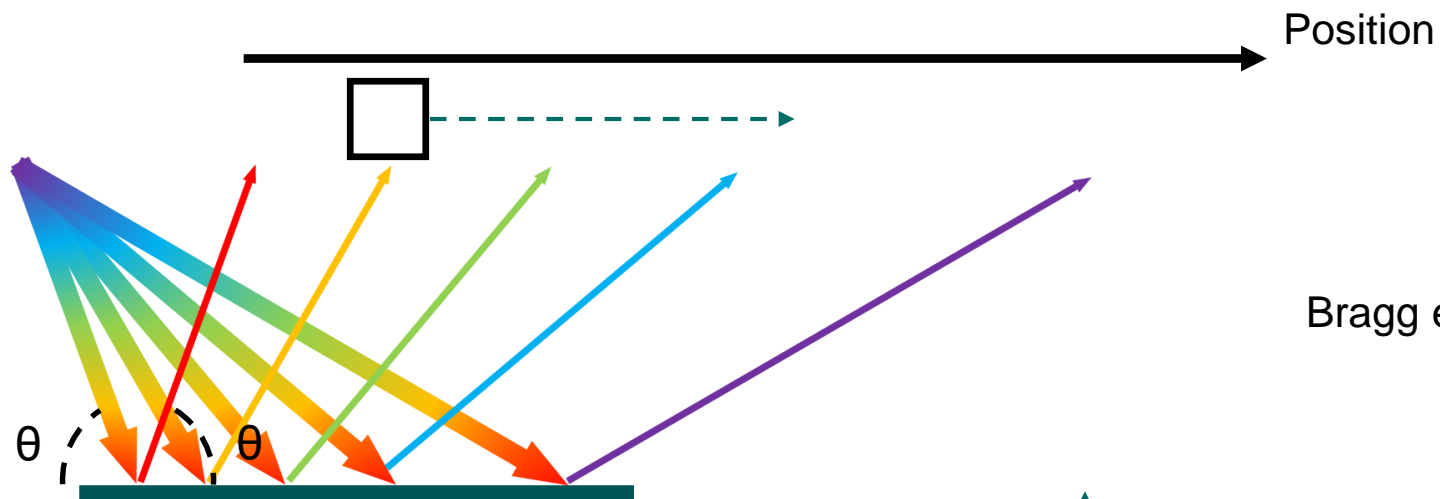
BLiX
Berlin Laboratory for
innovative X-ray Technologies

XAS

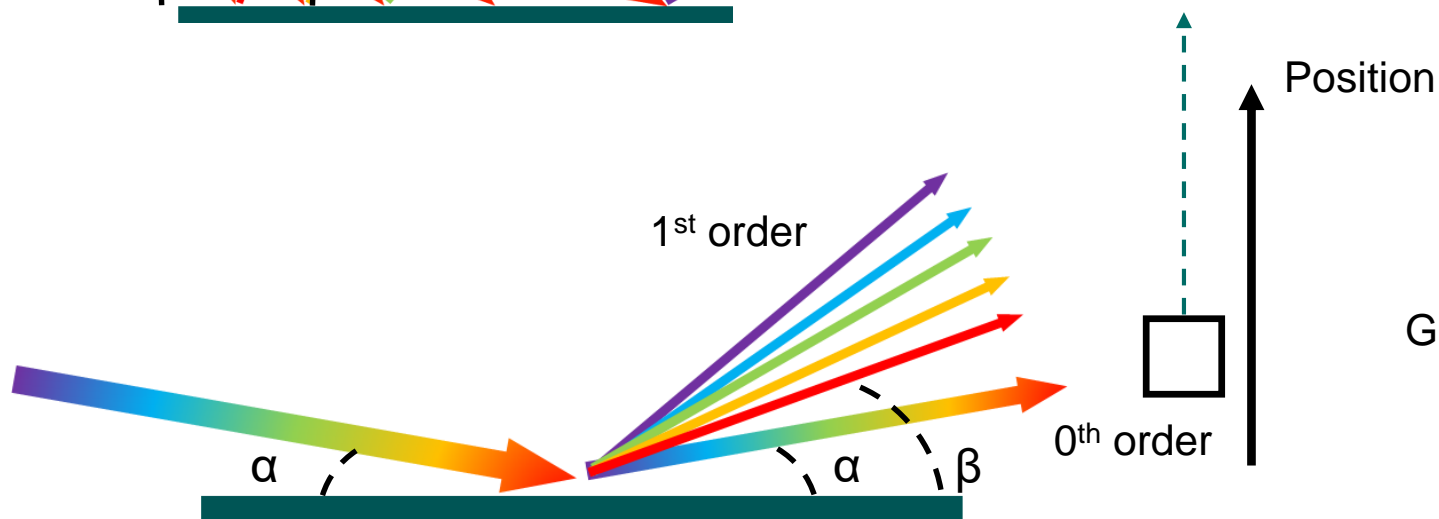
Soft X-ray
radiation

XANES
Hard X-ray
radiation

SCANNING-TYPE SPECTROMETERS

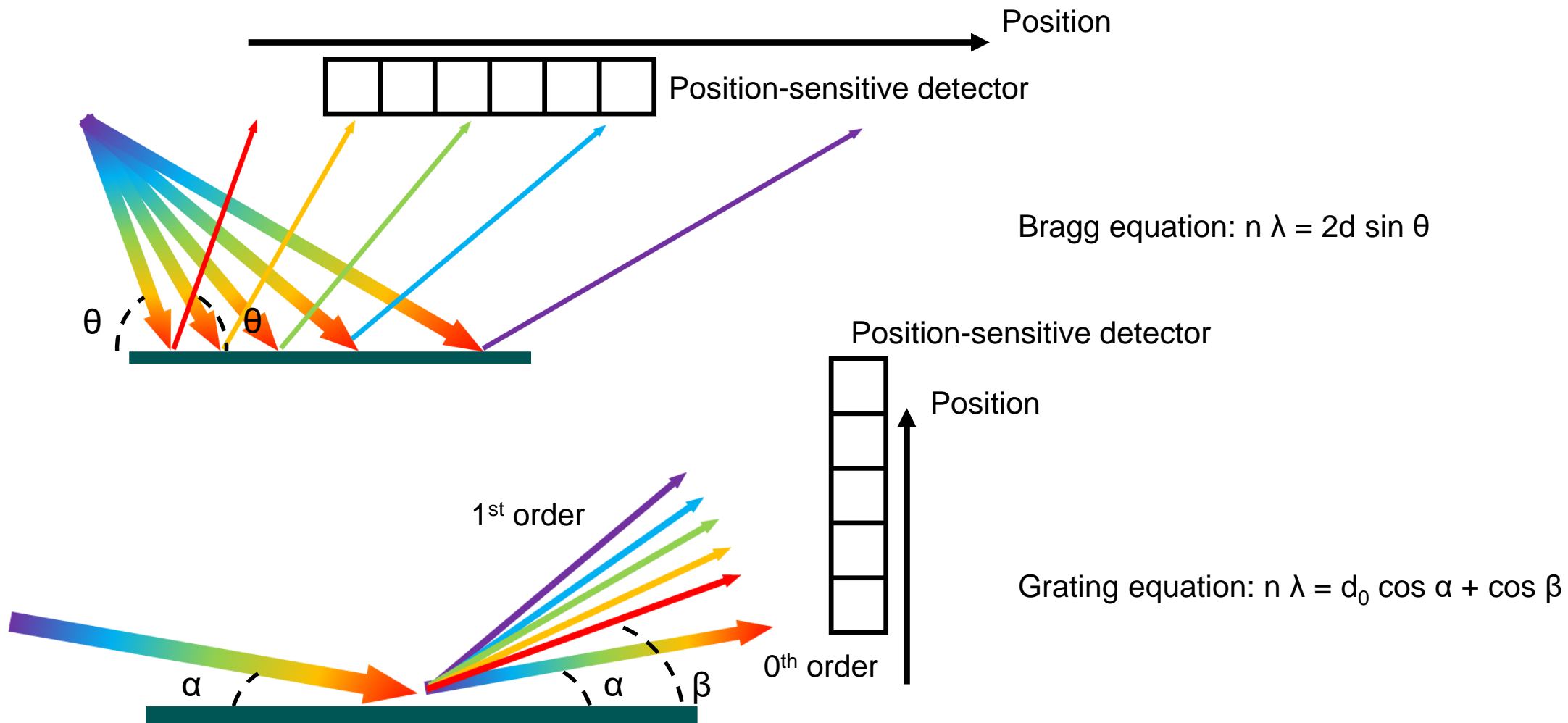


Bragg equation: $n \lambda = 2d \sin \theta$

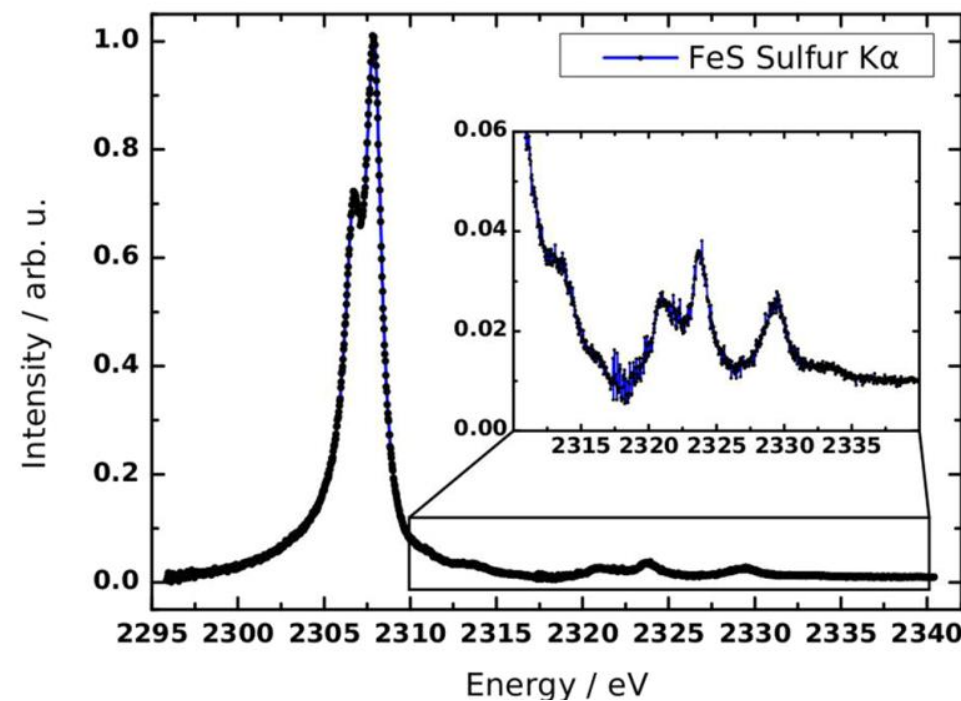
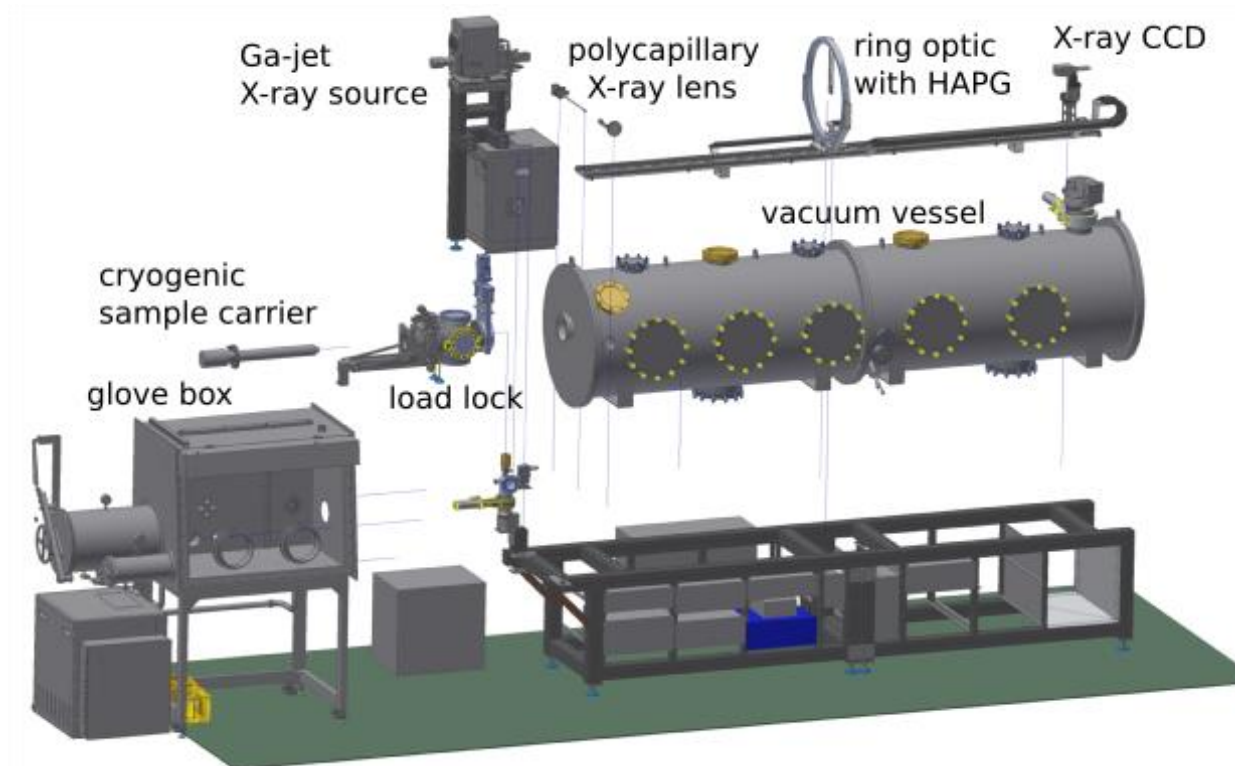


Grating equation: $n \lambda = d_0 \cos \alpha + \cos \beta$

DISPERSIVE-TYPE SPECTROMETER



FULL CYLINDER VON HAMOS X-RAY EMISSION SPECTROMETER



Rev Sci. Instrum. 89, 113111 (2018).

DETECTION SENSITIVITY CONSIDERATIONS

- Photon flux

Exp. determined photon flux for Ga K α : $6.0(5) \times 10^{12} \text{ s}^{-1} \text{ sr}^{-1}$ at 200 W for 68% Ga, 22% In and 10% Sn

J. Anal. At. Spectrom. 34, 1497 (2019).

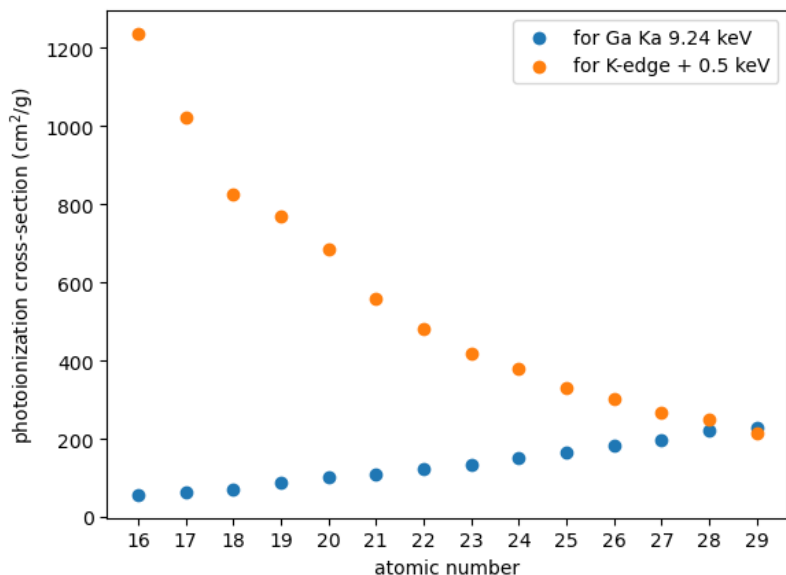
→ $1 \times 10^{10} \text{ s}^{-1}$ Ga K α photons (9.65 keV) at 250 W

- Impact of focusing optics

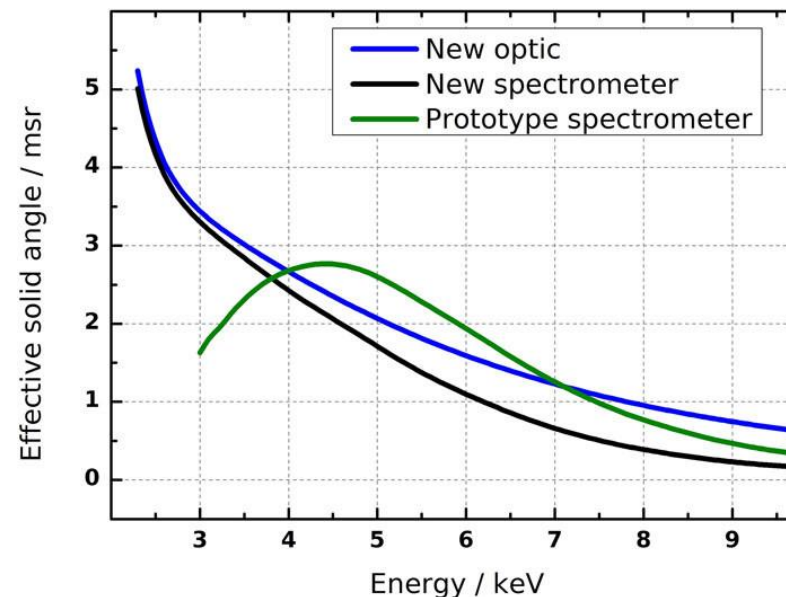
Modelled transmission and solid angle of acceptance reduce photon flux by a factor 10^{-3}

J. Anal. At. Spectrom., 36, 2519 (2021).

- Atomic fundamental parameters: photoionization cross-section, fluorescence yield, trans. prob.



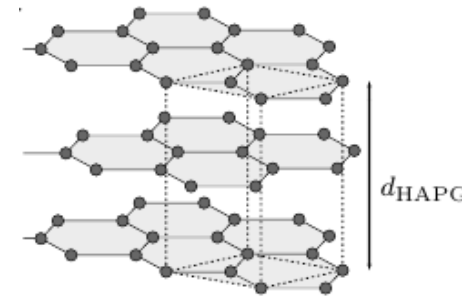
- Detection efficiency: solid angle of diffraction crystal, reflectivity, CCD efficiency



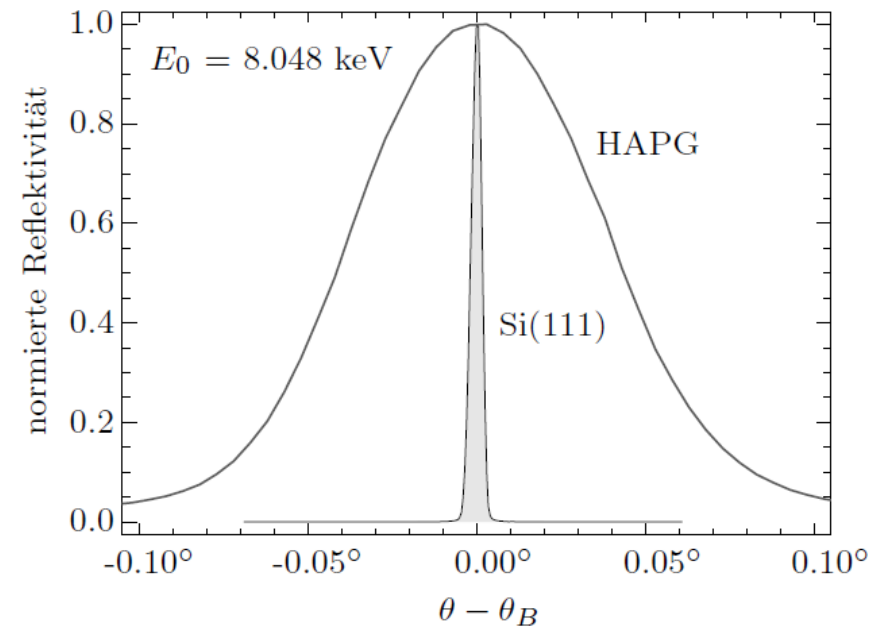
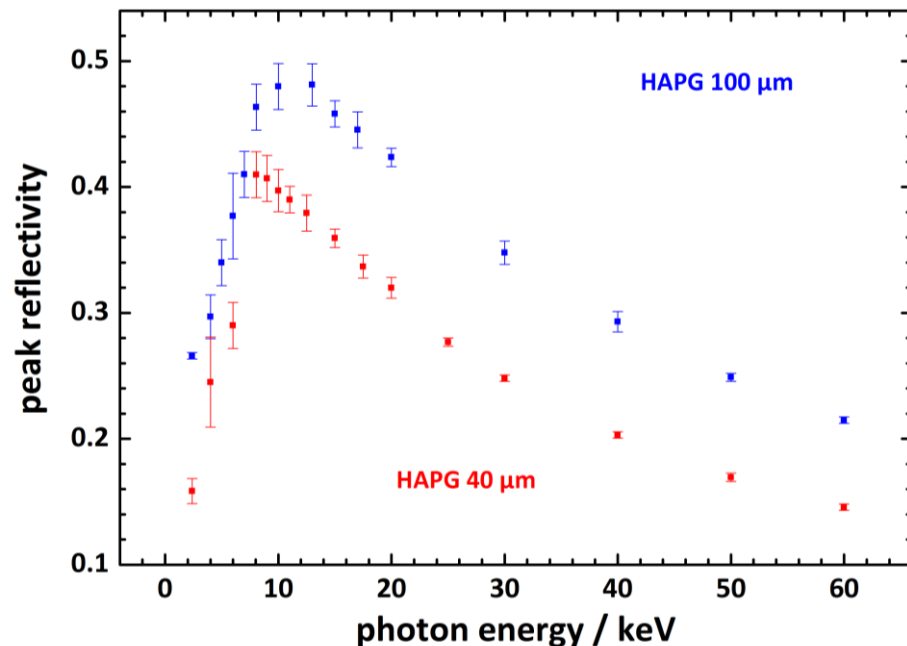
Rev Sci. Instrum. 89, 113111 (2018).

HIGHLY ANNEALED PYROLITHIC GRAPHITE

- mosaic crystal that has intrinsically a high integral reflectivity due to mosaic focusing
→ 5x times larger than that of pure crystals
- can be applied to optics with a small radius of curvature without lattice distortions
→ increased solid angle of detection can be realized

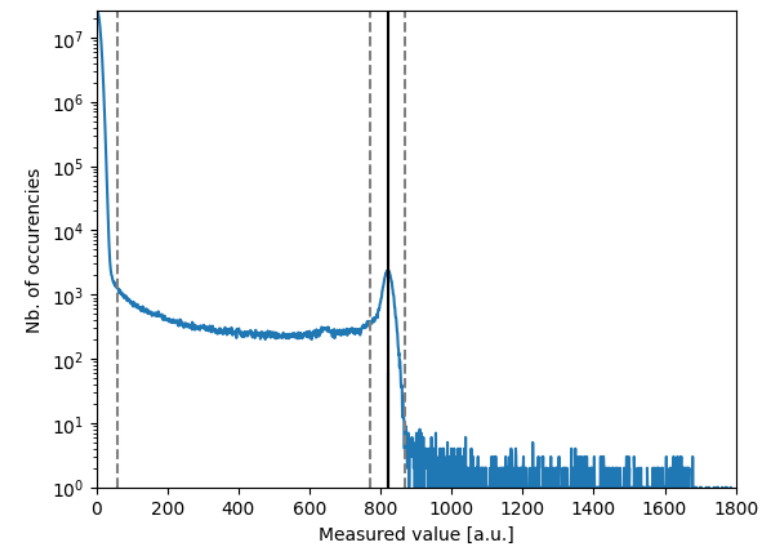
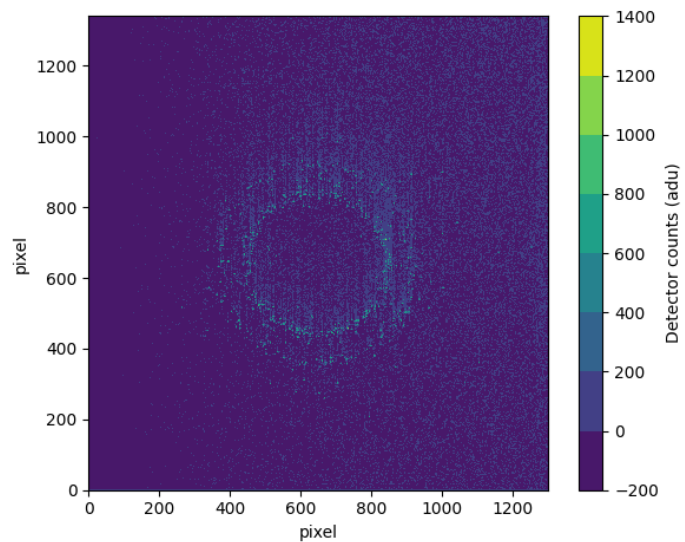


→ spectrometers with an increased detection efficiency can be realized

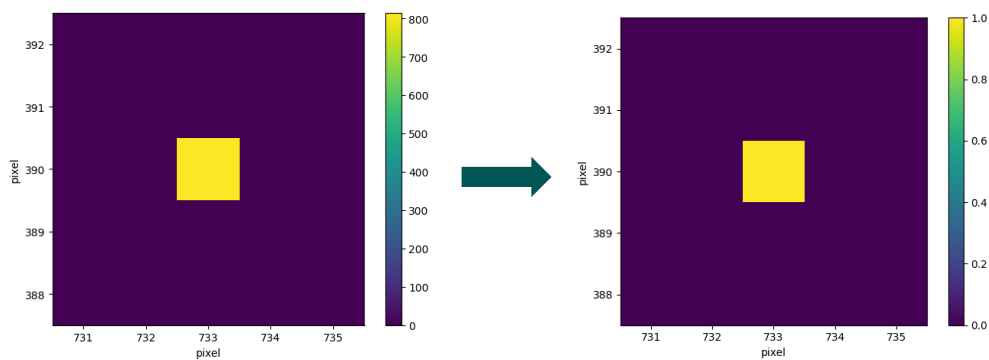


J. Appl. Cryst. 48, 1381-1390 (2015)

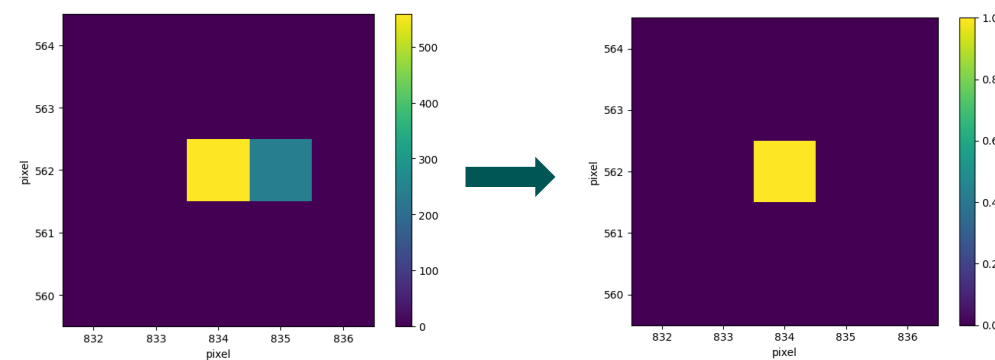
SINGLE PHOTON IMAGE EVALUATION



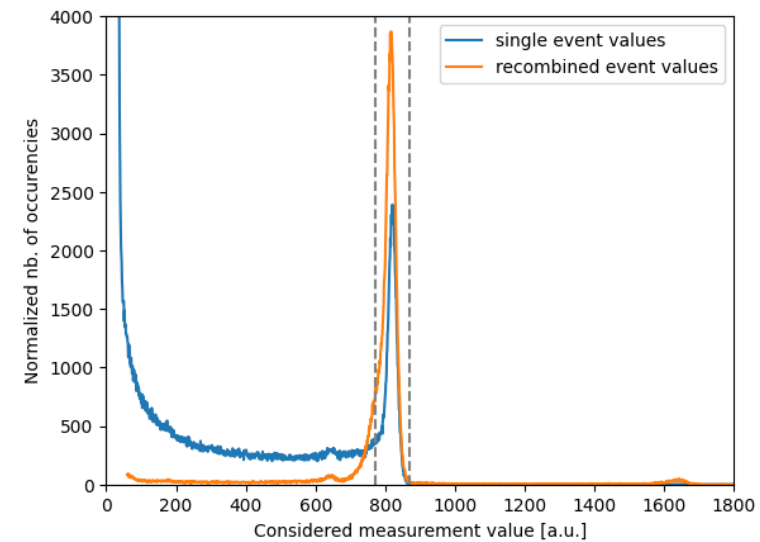
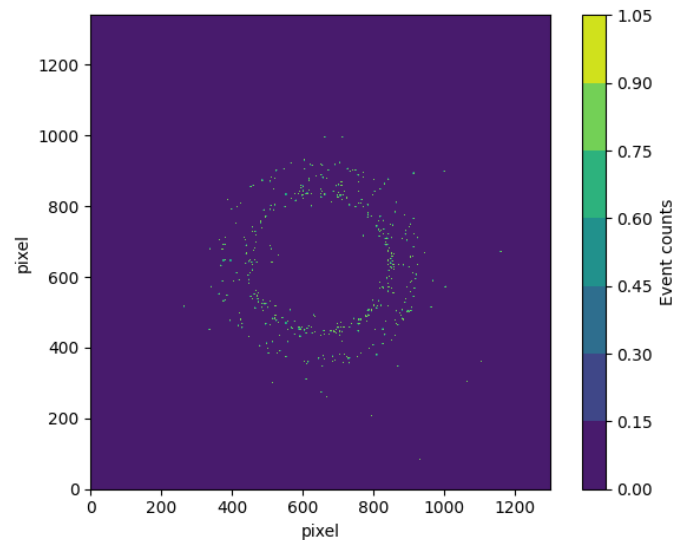
1 pixel event



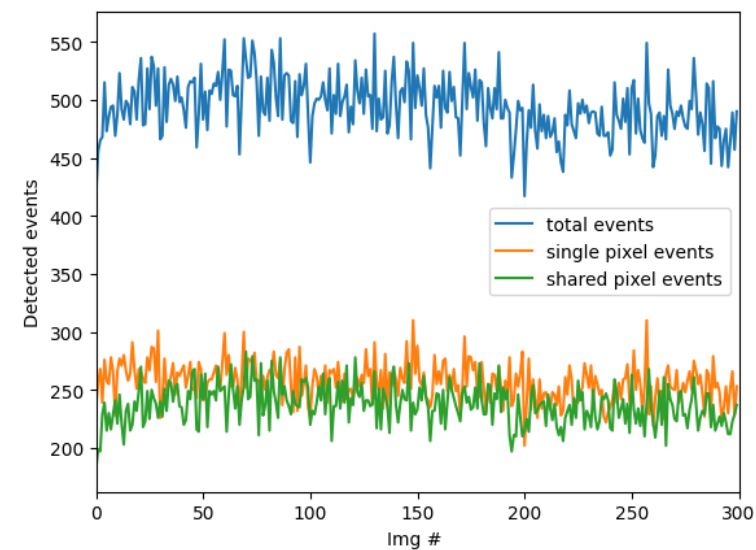
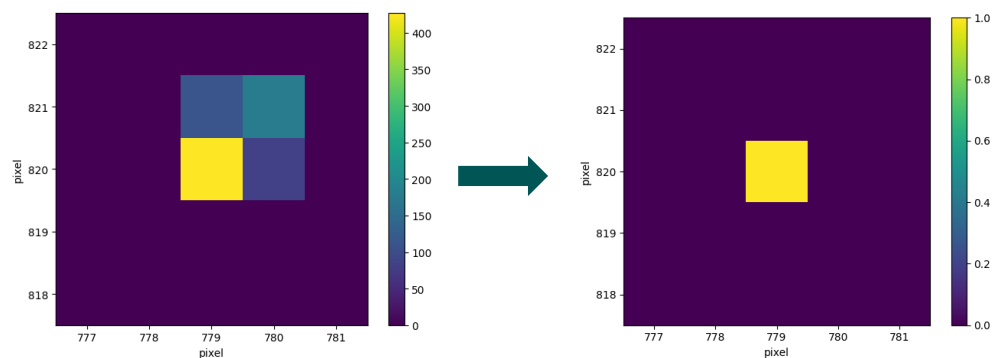
2 pixel event



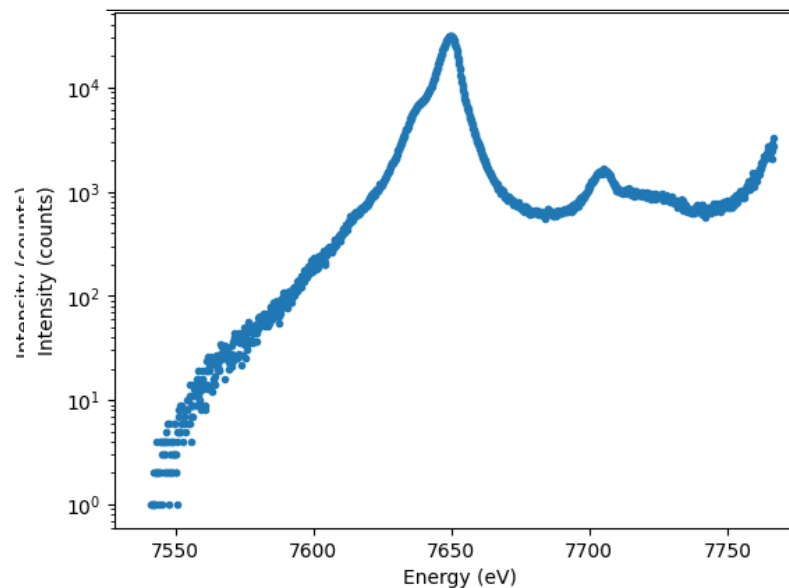
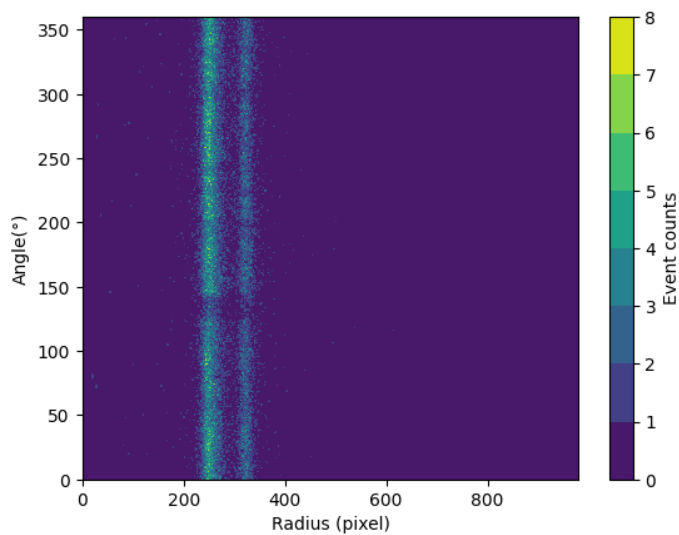
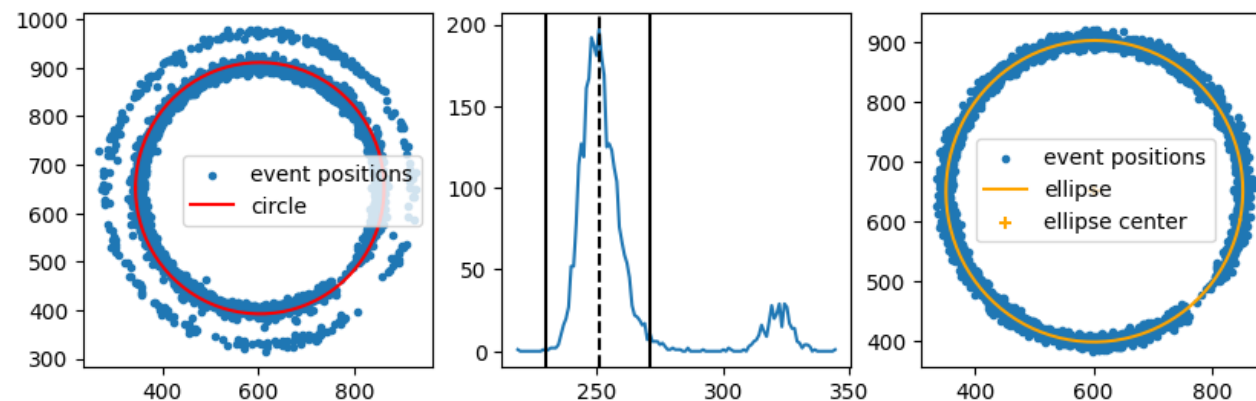
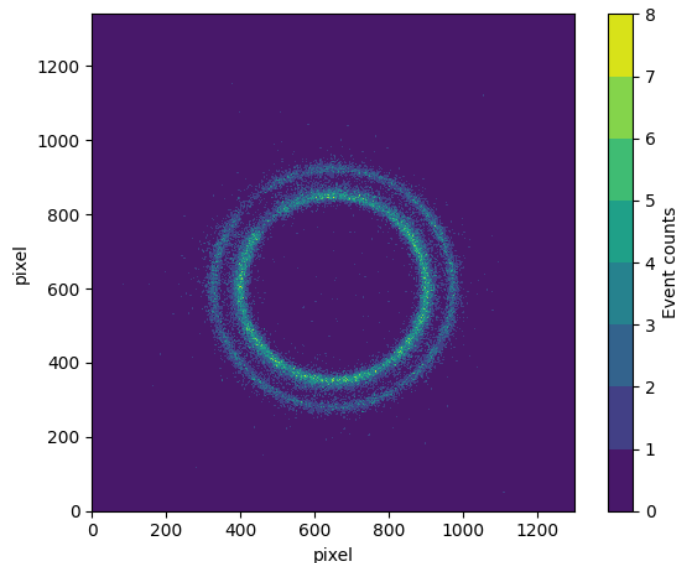
SINGLE PHOTON IMAGE EVALUATION



4 pixel event



FROM IMAGE TO SPECTRUM

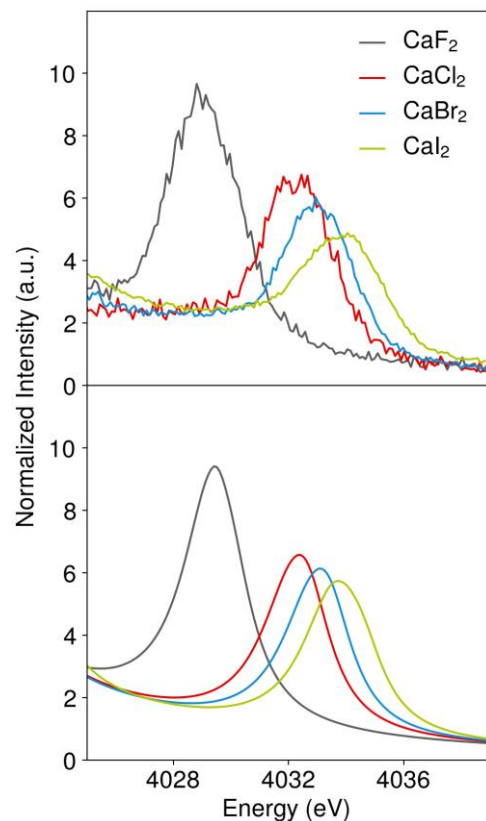


- Using a reference line, assign energy to radius
- change in measurement position, will result in change in radius
- at new position, assign radius to energy

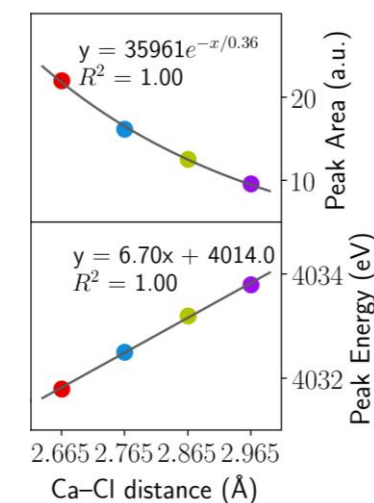
CALCIUM VALENCE-TO-CORE XES

Calculations with artificial Ca–Cl distances help understand structure–spectrum relationships

- Energy depends on the electronegativity / intrinsic ionisation energy of the ligand
- Peak areas increase exponentially as distance becomes shorter
- Peak energies decrease linearly as distance shortens

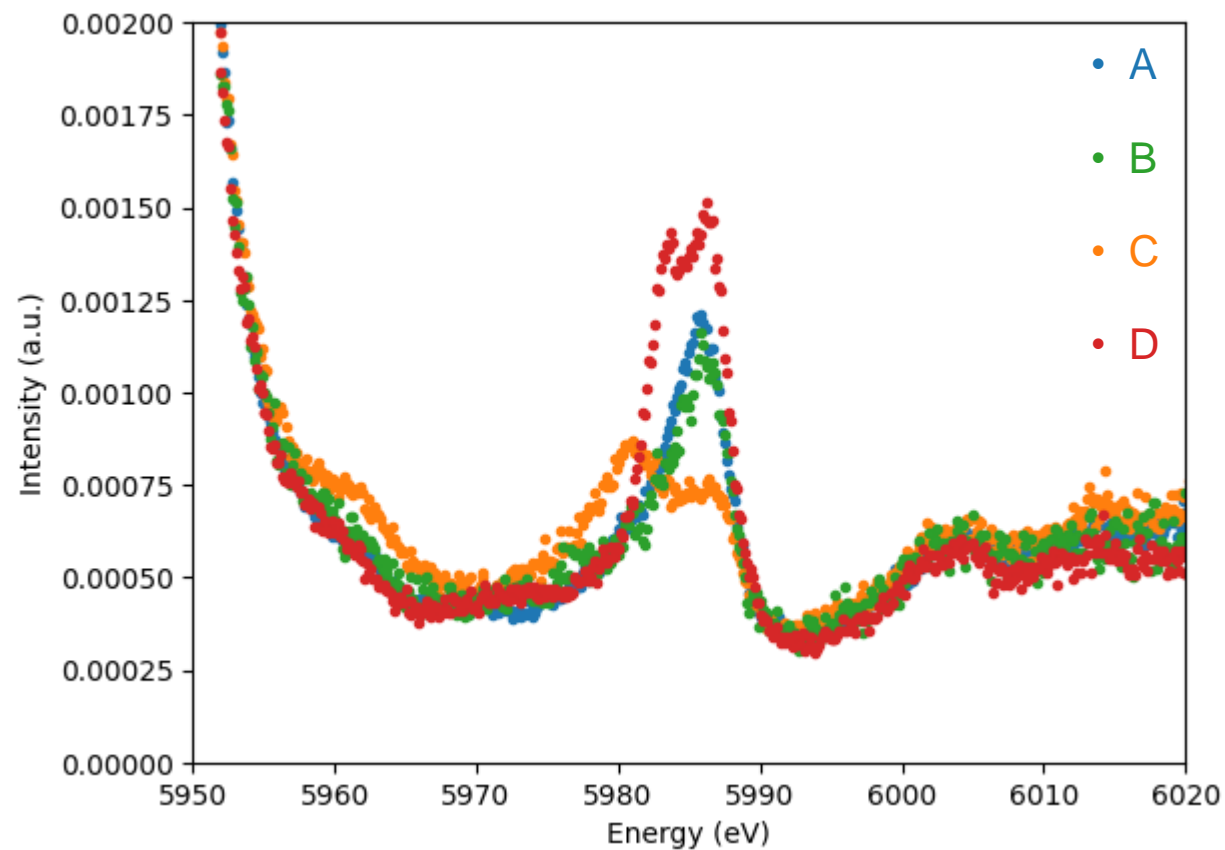
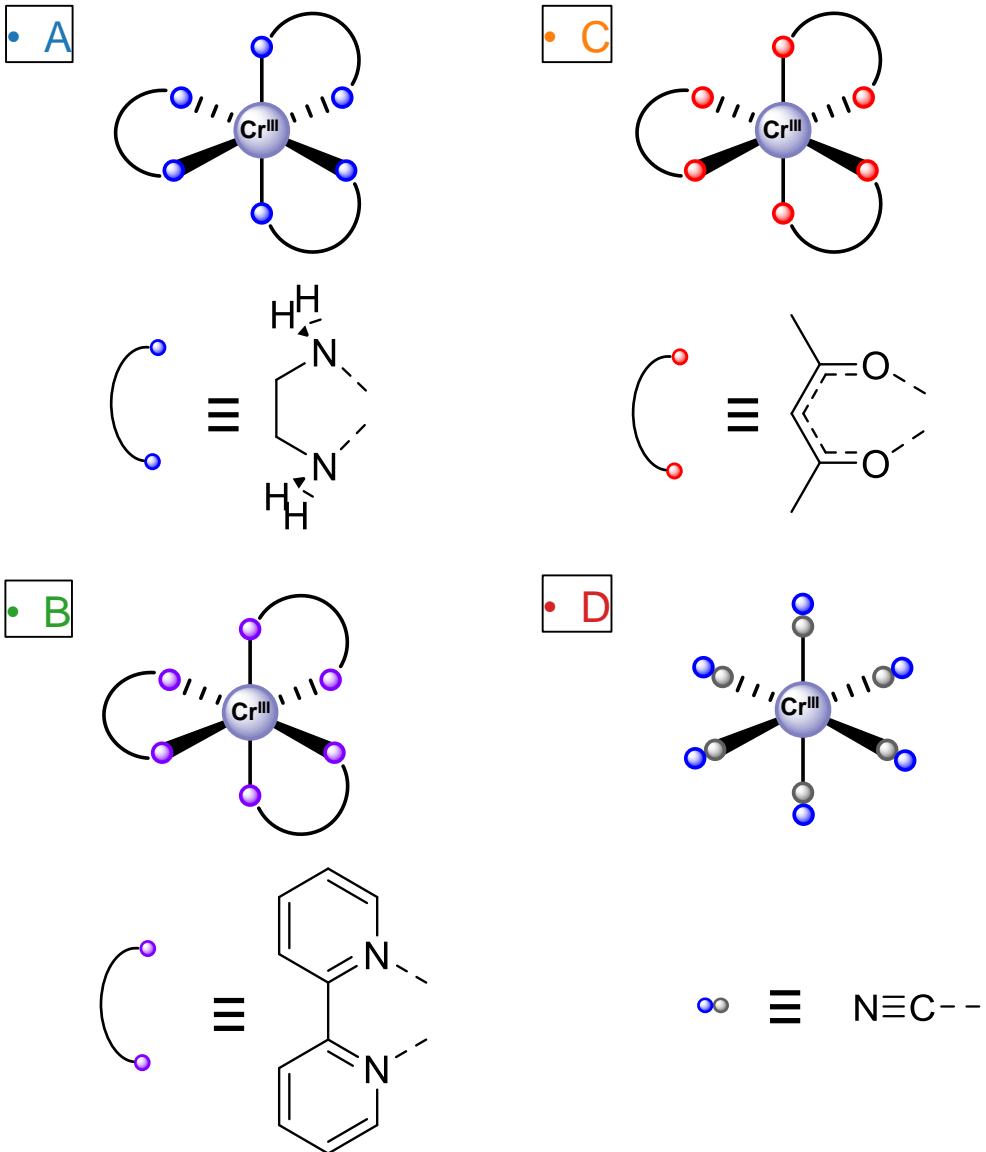


Compound	Coordination	Halogen Pauling Electronegativity	Average Ca–X Distance (Å)
CaF ₂	8 (O _h)	3.98	2.366
CaCl ₂	6 (O _h /D _{4h})	3.16	2.745
CaBr ₂	6 (O _h /D _{4h})	2.96	2.885
CaI ₂	6 (O _h)	2.66	3.117



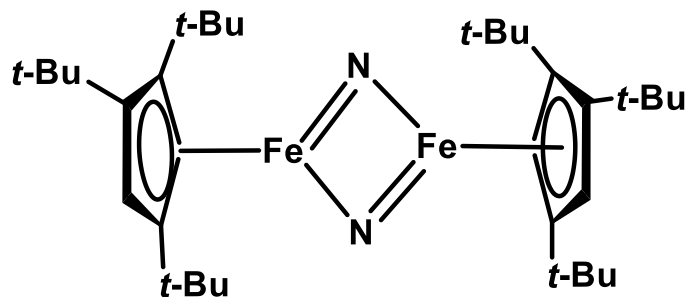
Inorg. Chem. 58, 16292 (2019).

ELECTRON-/ENERGY-TRANSFER PHOTOCHEMISTRY

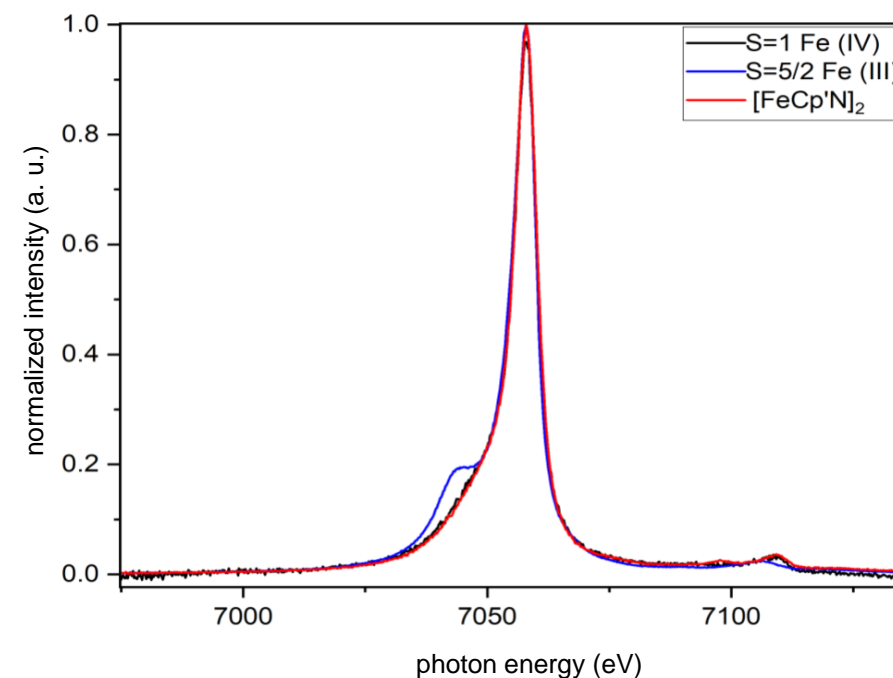


Courtesy of Issiah B. Lozada

INVESTIGATION OF IRON DIMERS

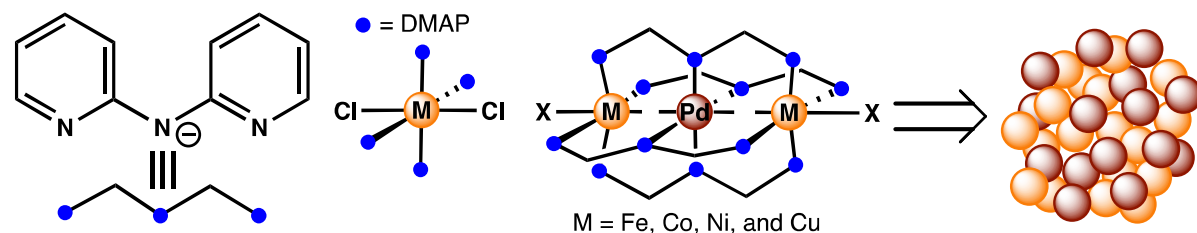


- Fe centers, supported by substituted cyclopentadiene bridging nitride groups.
- the Fe atoms are coupled with strong antiferromagnetic interactions
→ diamagnetic behavior by the system
- determination of oxidation states by widely employed magnetometric techniques like SQUID is complicated



Courtesy of Vishwashri Srinivasan

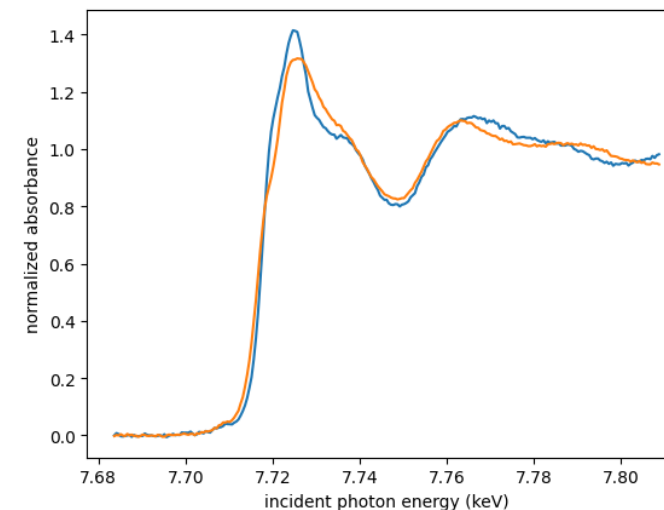
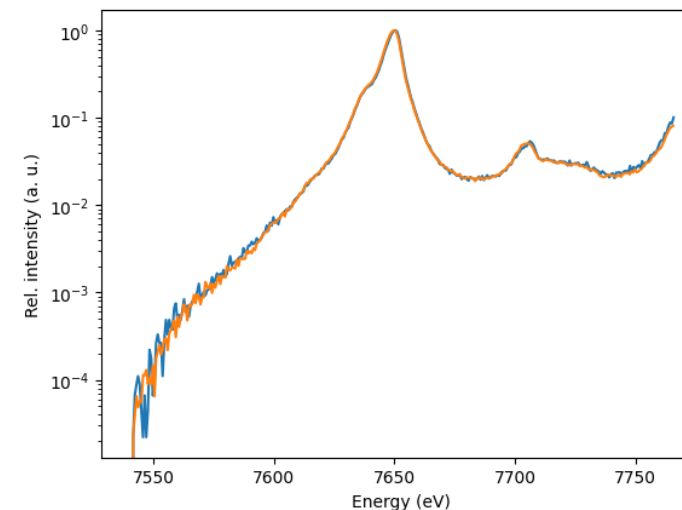
DIRECT H₂O₂ SYNTHESIS FROM H₂ AND O₂



- Concentration of H₂O₂ produced limited by concentration of H₂/O₂ in gas mixture (explosive risk)
- Interest in on-site production and consumption
- > 95% selectivity (Au-Pd, Sn-Pd)
> 99% H₂ utilization (Au-Pd, Sn-Pd)
- H₂O₂ decomposition by catalyst must be minimized
- Productivity and H₂O₂ degradation rate modified via introduction of secondary metals and support material
- Goal: Understand effects of secondary metals on the electronic structure of Pd and which effects are beneficial towards catalysis.

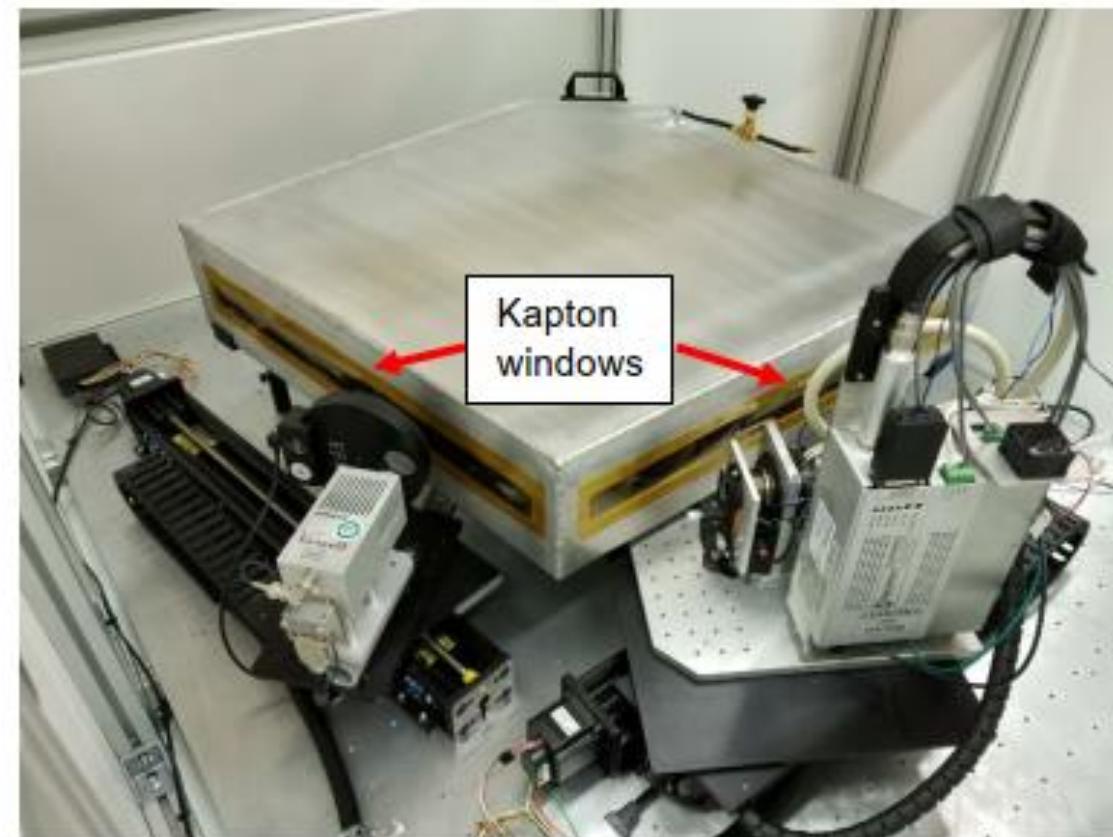
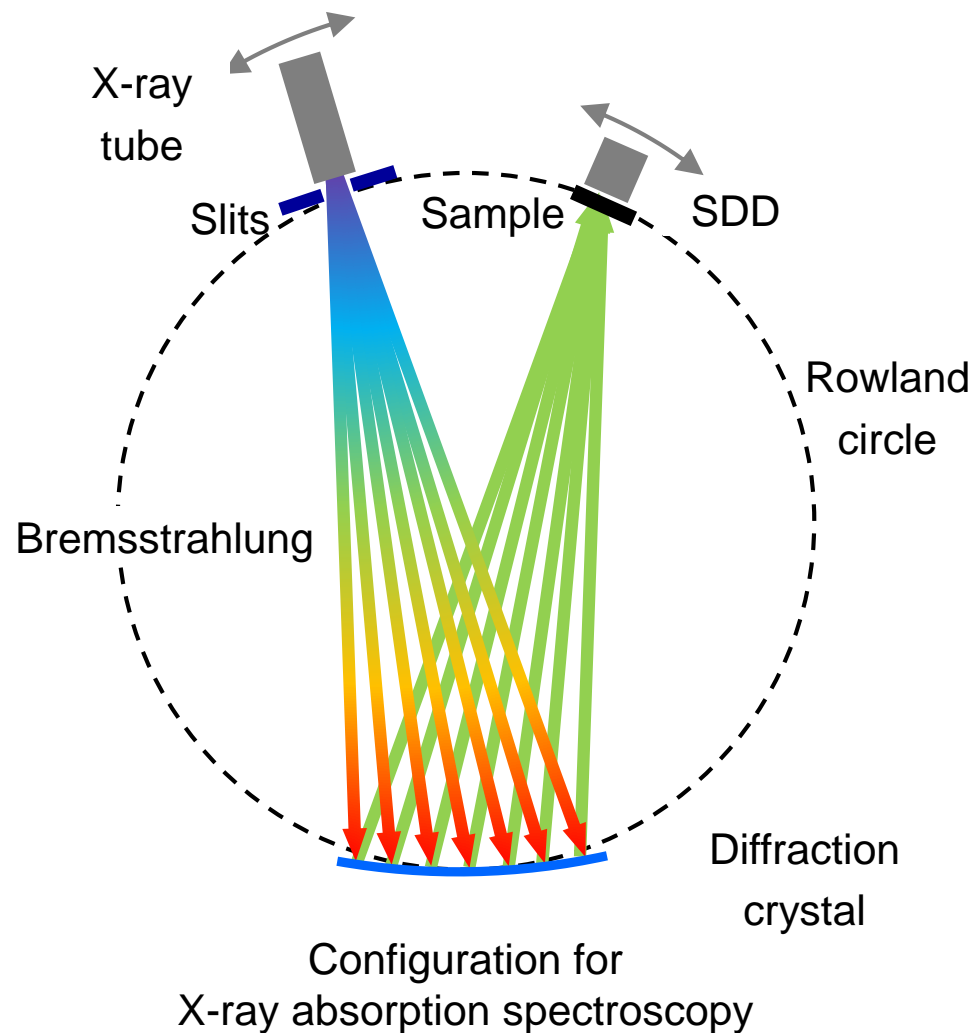
MCl₂(pyridine)₄ (M = Co)

MPdM complexes (M = Co)



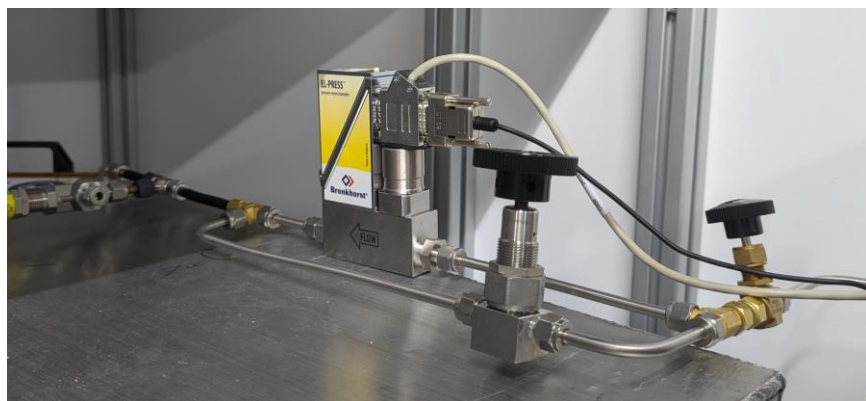
Courtesy of Anna G. Scott

EASYXES-100 SETUP DEVELOPMENT

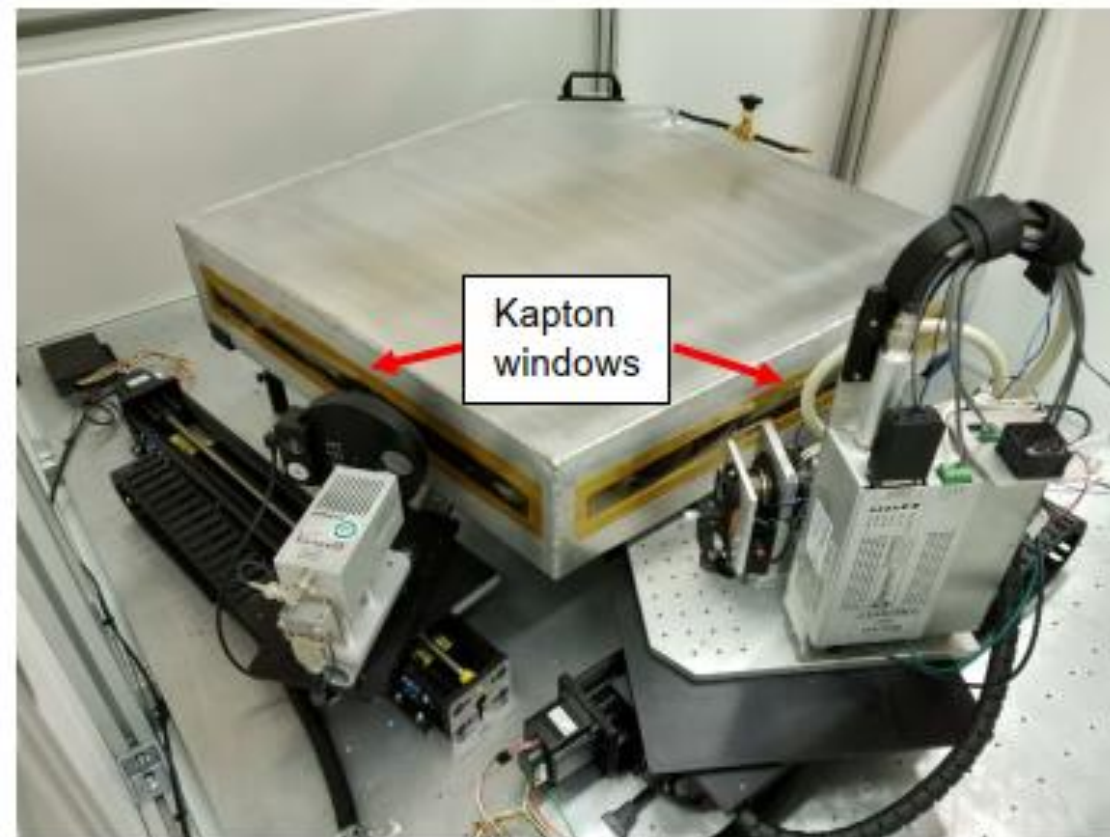


Rev. Sci. Instrum. 90, 024106 (2019).

EASYXES-100 SETUP DEVELOPMENT



Automatized overpressure regulation on the He flowbox

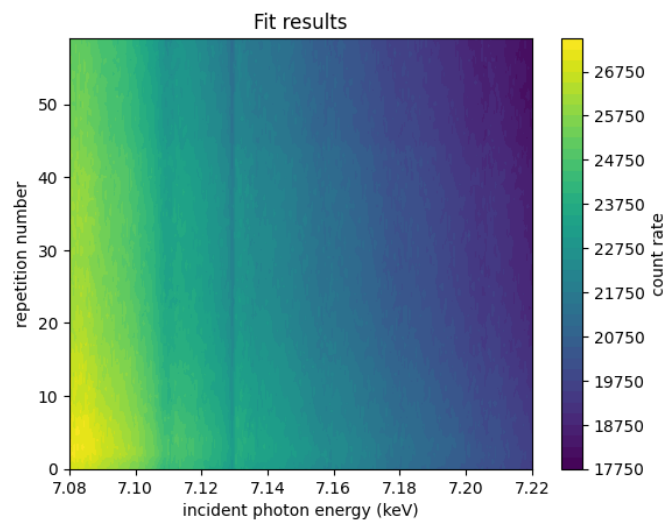


Rev. Sci. Instrum. 90, 024106 (2019).

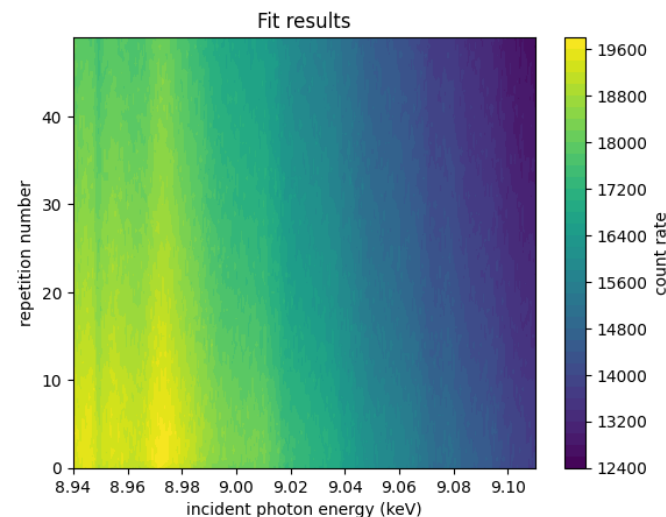
SETUP DEVELOPMENT ON EASYXES-100 INSTRUMENT

without automatized overpressure regulation

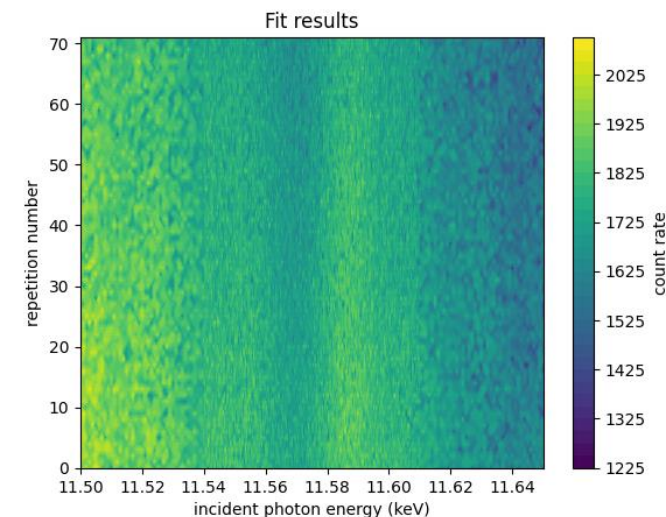
Fe K



Cu K

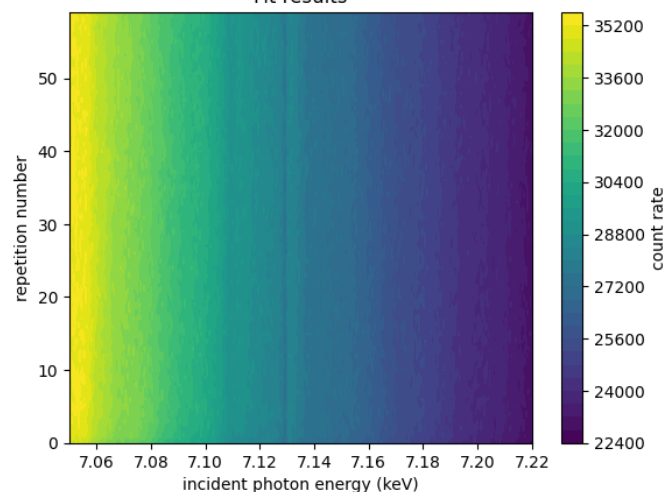


Pt L₃

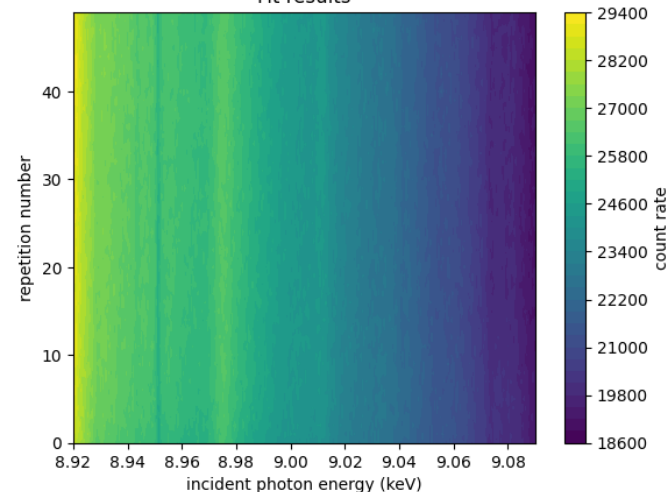


with automatized overpressure regulation

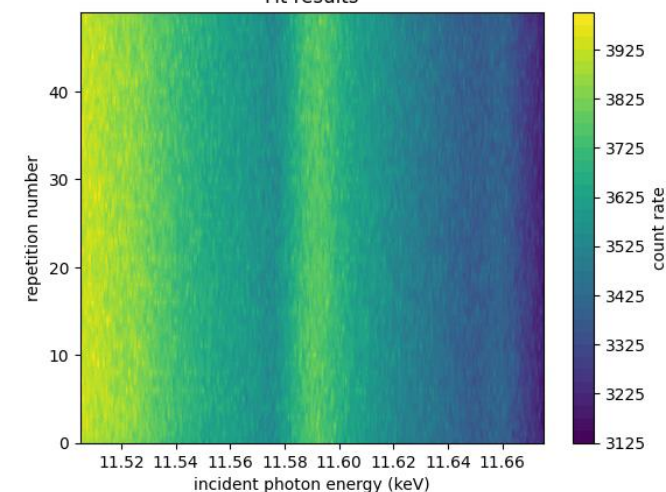
Fit results



Fit results

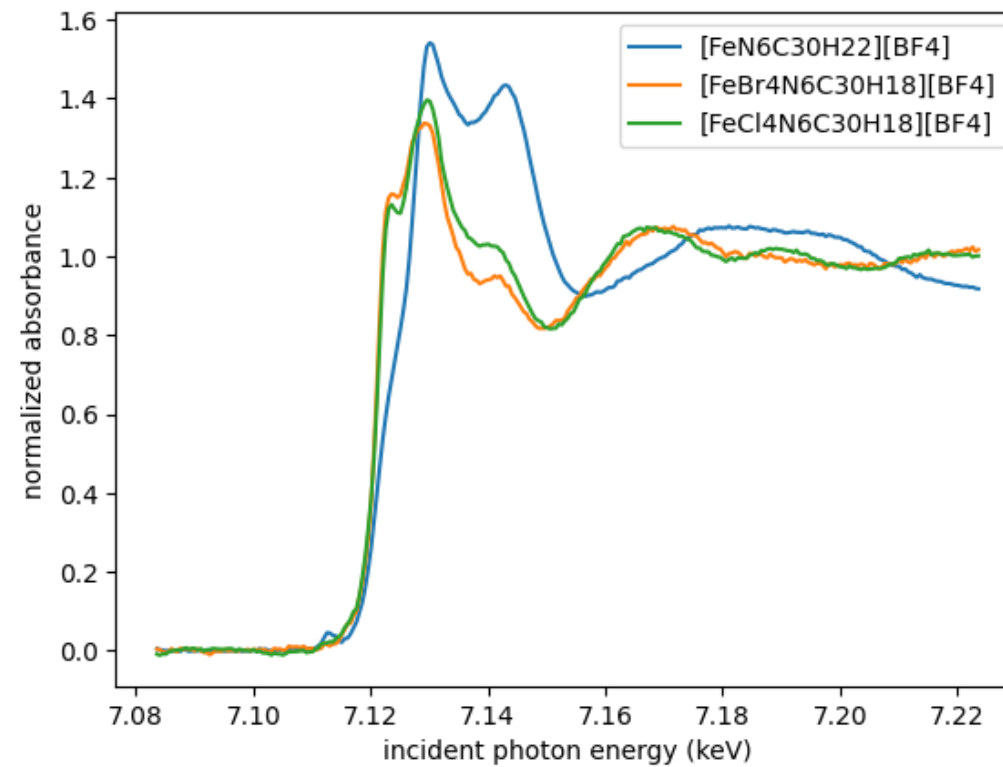


Fit results



XANES MEASUREMENTS

Interlaboratory comparison



LABXANES INSTRUMENT

source

Liquid metal jet as a high-power micro-focused X-ray source

optic

Cylindrically curved Si or Ge crystals

Cuts with forbidden 2nd diffraction order

detector

Single-photon counting EIGER2R hybrid CMOS 2D pixelated detector

fast readout & position sensitive detection

setup

Slitless geometry

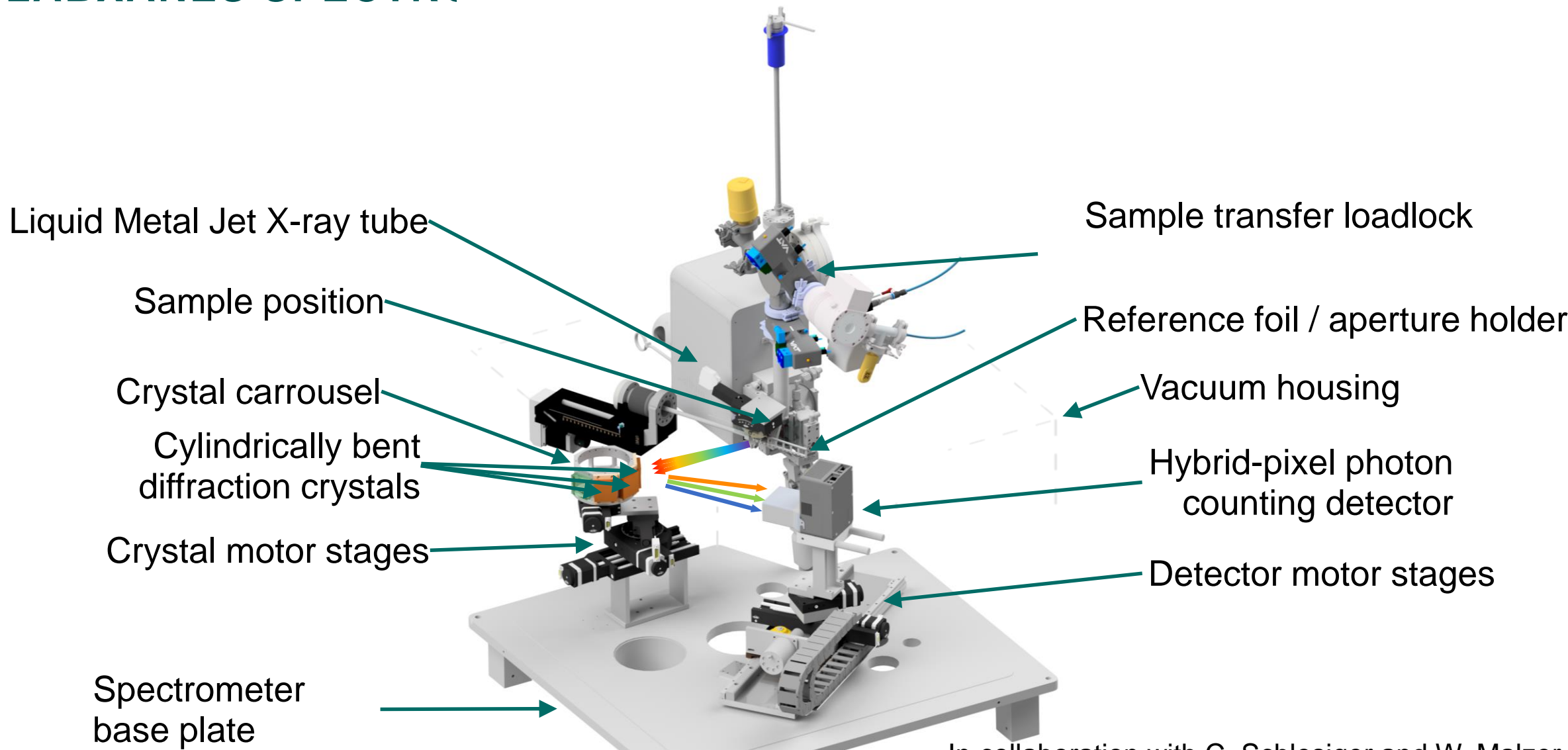
Peltier element for sample cooling or heating

characteristics

Technique(s)	XANES
Type	Dispersive
Geometry	von Hamos (R = 350 mm)
Source	Metal-Jet X-ray tube
Dispersive Element	cylidnricaly crved Si or Ge crystals
Detector	Eiger
Energy range	5 keV - >11 keV
K edges	Ti → Zn
L edges	Cs → Ir
Sample Cooling	Yes (Peltier)
Options	-
Energy window	> 0.2 keV
Resolving power E/ΔE	> 4000
Measurement time	to be commissioned

In collaboration with C. Schlesiger and W. Malzer

LABXANES SPECTROMETER

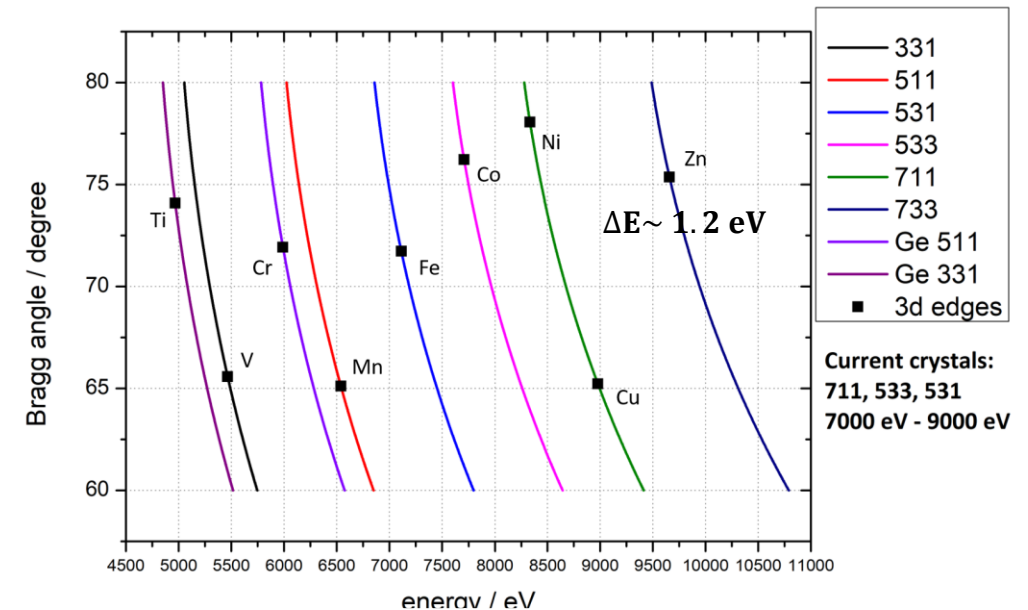


In collaboration with C. Schlesiger and W. Malzer

DESIGN PERFORMANCE

Considerations on crystal selection

- selection of crystal cuts: measurement at high Bragg angle ($n \cdot hc/E = 2d \sin \theta \rightarrow \Delta E/E = \cot \theta \Delta \theta$)
- pure Si or Ge crystals: better resolving power, but lower reflectivity compared to synthetic or mosaic diffraction crystals
- radius of curvature R : impacts solid angle of detection ($\Omega \sim 1/R^2$) and resolving power ($\Delta E/E \sim 1/R$)
- crystal cuts with forbidden 2nd diffraction order: allows using fast read-out detectors without energy discrimination capabilities



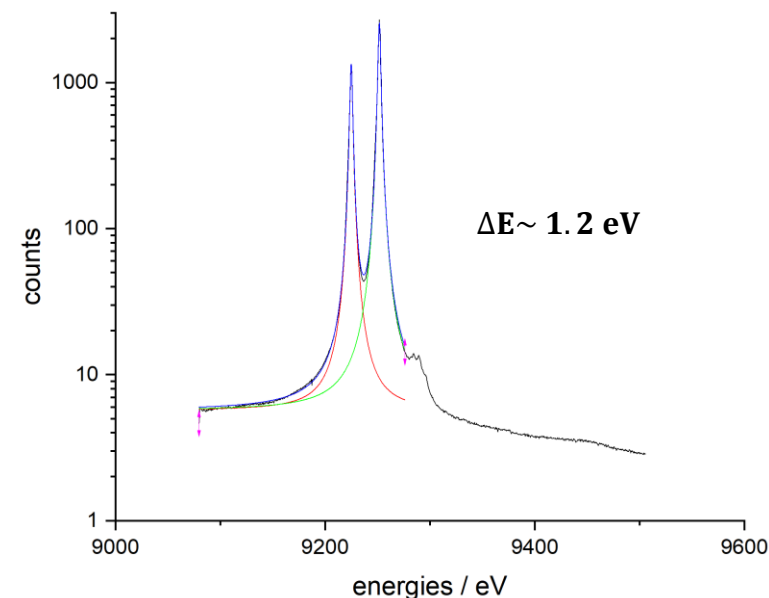
	Bragg angle	source contr.	crystal contr.	detector contr.	overall ΔE	energy range
Fe-K (7112 eV) @ Si 531	71.2°	0.13 eV	1.23 eV	0.24 eV	1.26 eV	278 eV
Ni-K (8333 eV) @ Si 533	63.9°	0.21 eV	1.73 eV	0.39 eV	1.79 eV	432 eV
Ni-K (8333 eV) @ Si 711	78.0°	0.10 eV	1.15 eV	0.18 eV	1.17 eV	222 eV
Cu-K (8979 eV) @ Si 711	65.2°	0.22 eV	2.20 eV	0.40 eV	2.26 eV	448 eV

In collaboration with C. Schlesiger and W. Malzer

DESIGN PERFORMANCE

Estimated resolving power and energy range covered

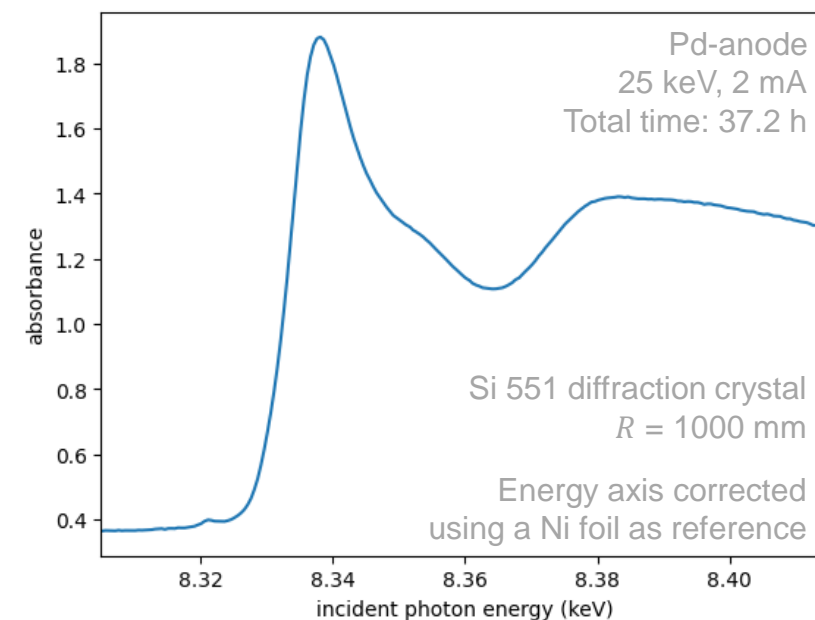
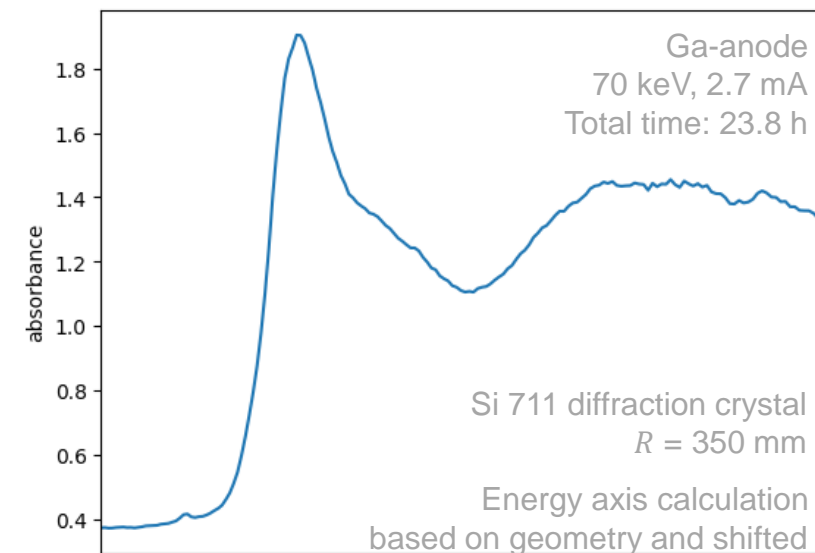
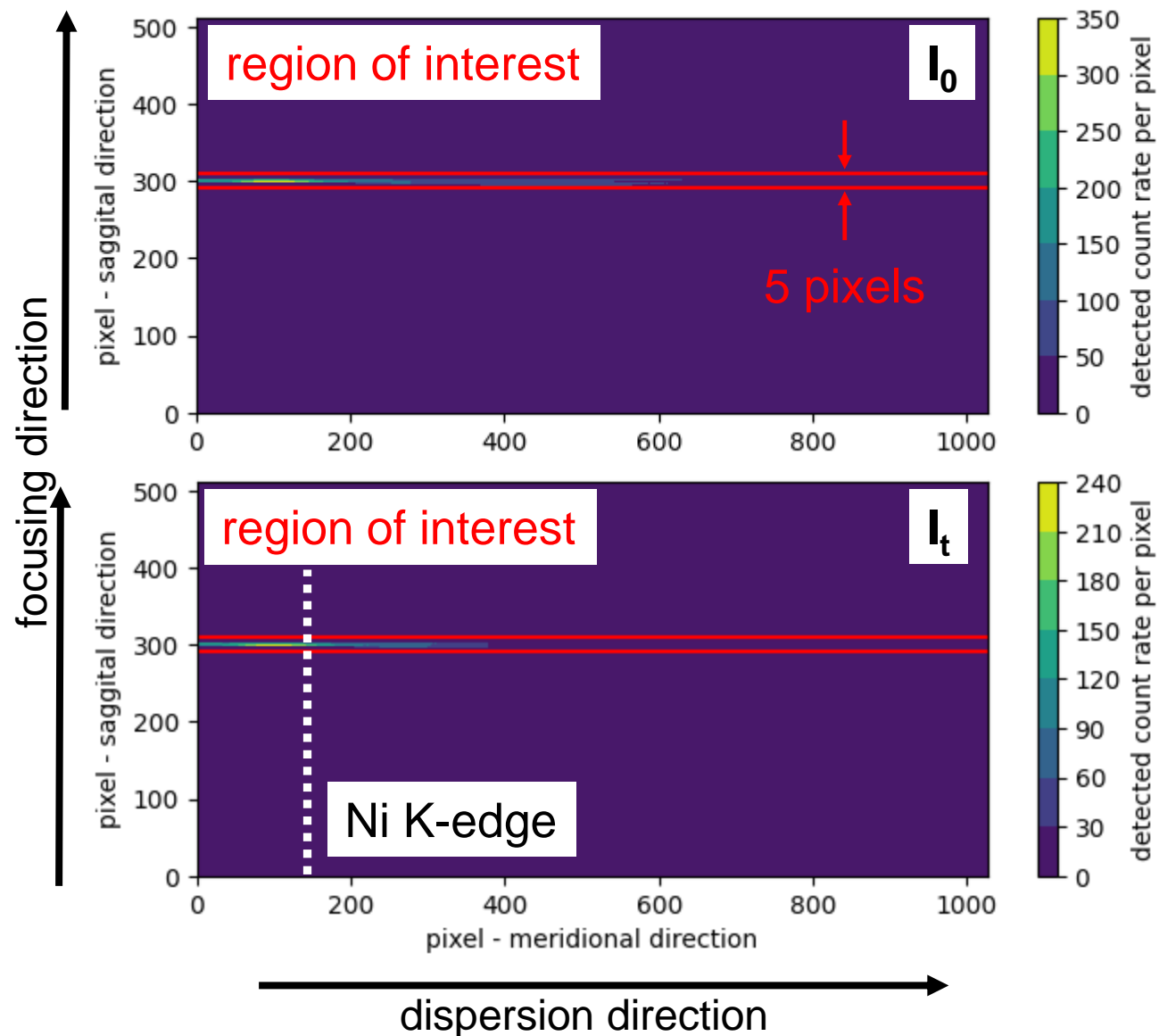
- source size ($s = 20 \mu\text{m}$) of the liquid metal jet: $\Delta E/E = s \cos \theta / R$
- crystal ($R = 350 \text{ mm}$, $d = 300 \mu\text{m}$): stress-strain and penetration depth effects calculated using pyTTE [A.-P. Honkanen and S. Huotari, IUCrJ 8, 102 (2021)]
- detector pixel size ($p = 75 \mu\text{m}$) in dispersion direction: $\Delta E/E = p \cos \theta / 2R$
- energy range covered defined by crystal and detector dimensions in dispersion direction



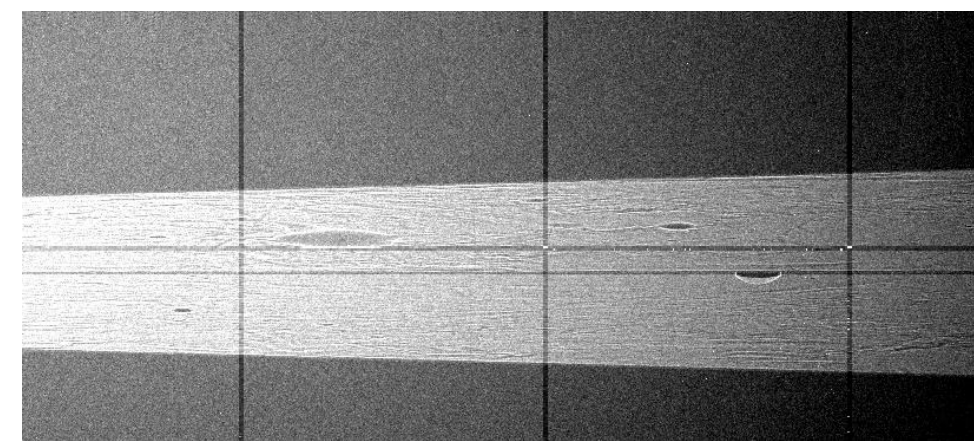
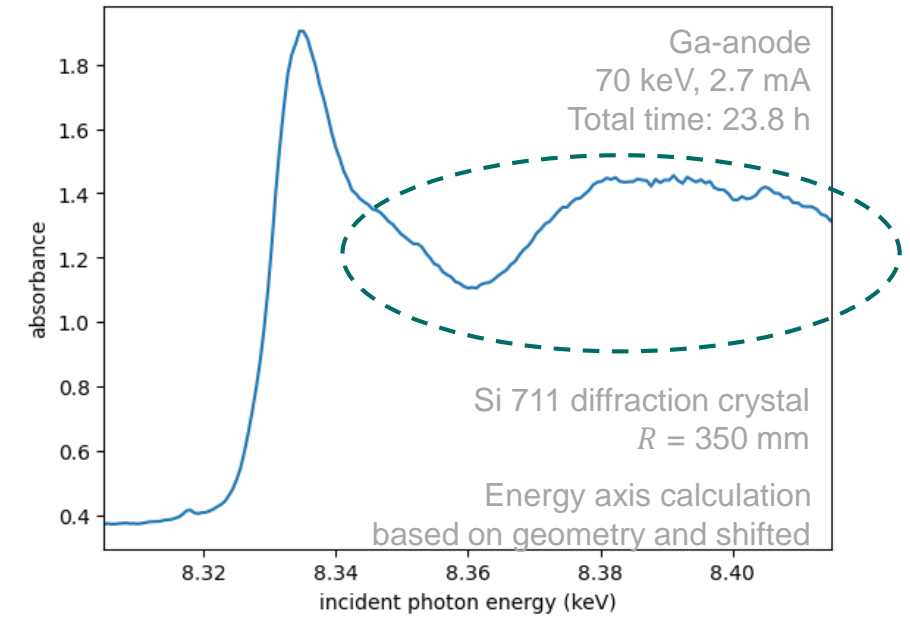
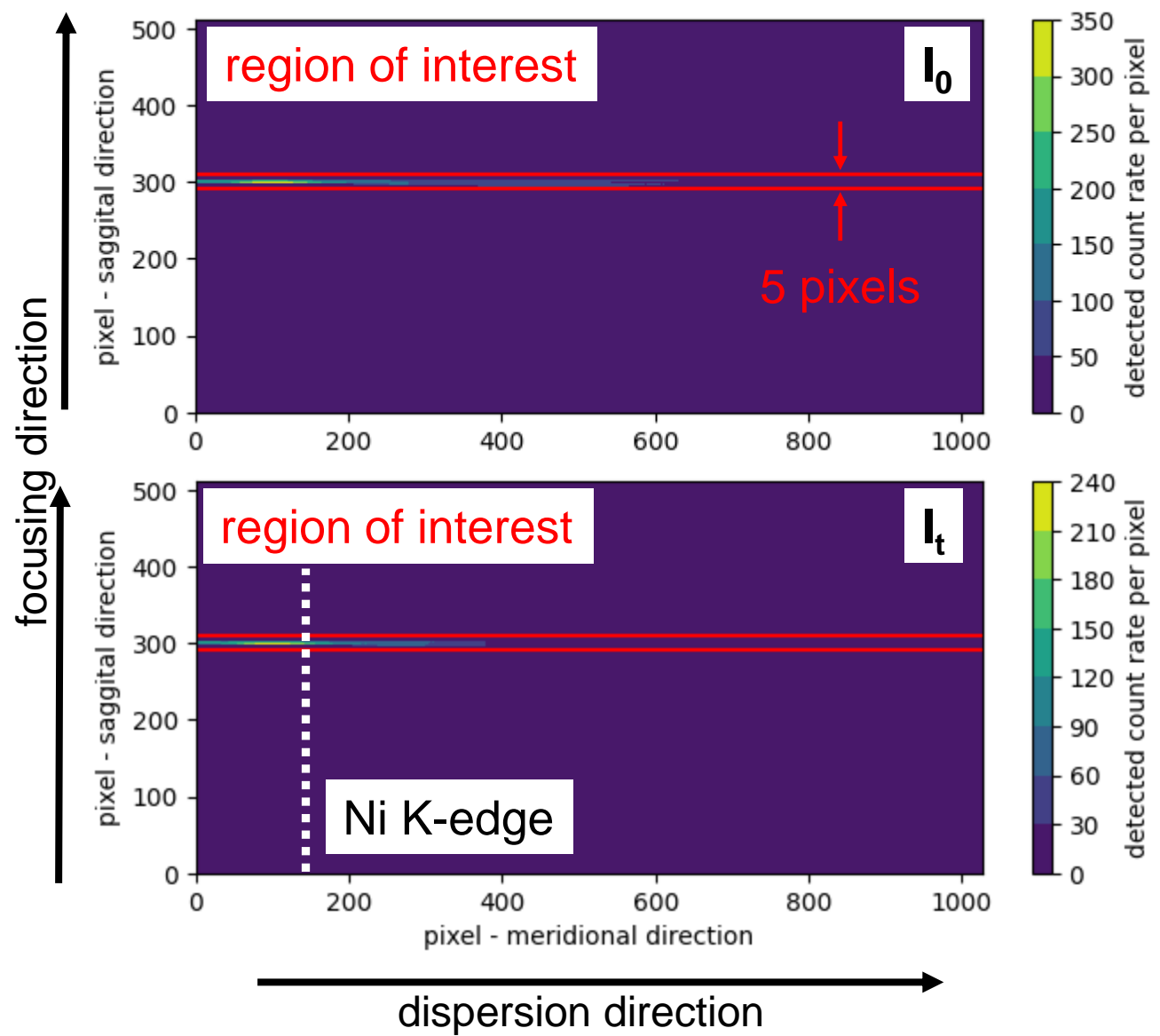
	Bragg angle	source contr.	crystal contr.	detector contr.	overall ΔE	energy range
Fe-K (7112 eV) @ Si 531	71.2°	0.13 eV	1.23 eV	0.24 eV	1.26 eV	278 eV
Ni-K (8333 eV) @ Si 533	63.9°	0.21 eV	1.73 eV	0.39 eV	1.79 eV	432 eV
Ni-K (8333 eV) @ Si 711	78.0°	0.10 eV	1.15 eV	0.18 eV	1.17 eV	222 eV
Cu-K (8979 eV) @ Si 711	65.2°	0.22 eV	2.20 eV	0.40 eV	2.26 eV	448 eV

In collaboration with C. Schlesiger and W. Malzer

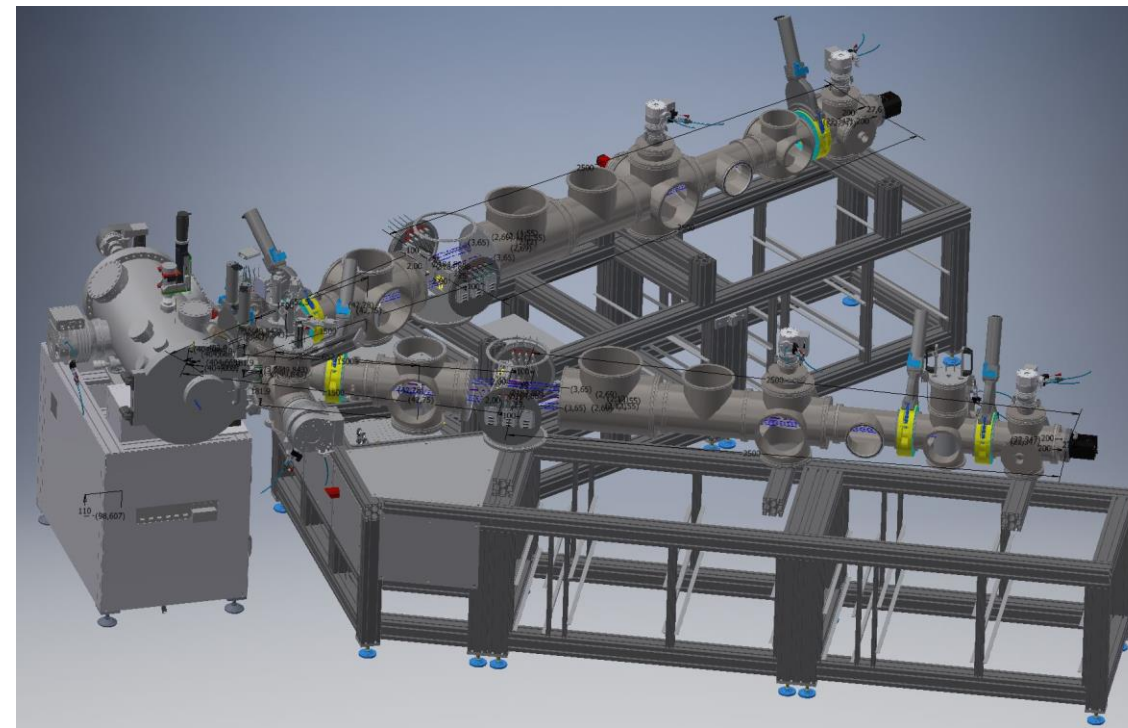
LABXANES OPERATION



LABXANES OPERATION

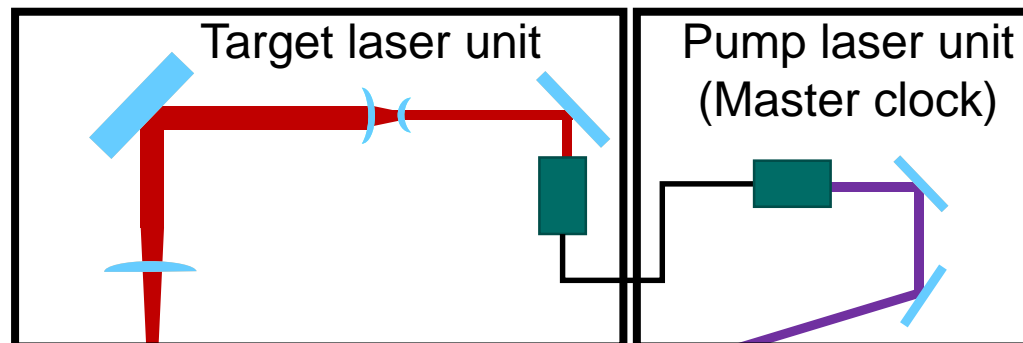
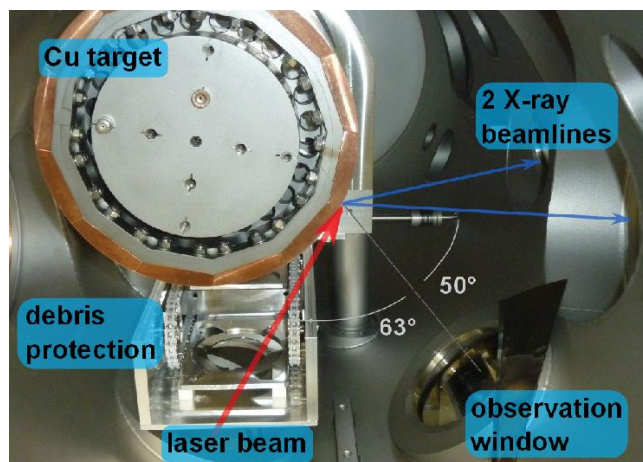


LPP SOURCE WITH 2 TWIN-ARM RZP SPECTROMETERS

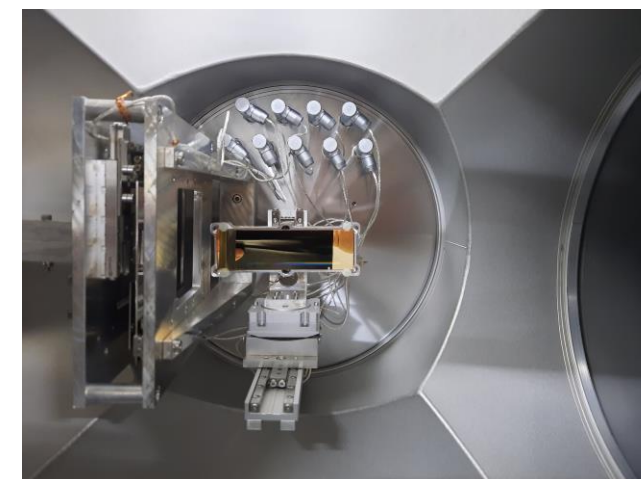
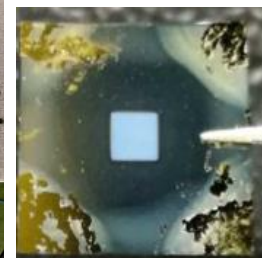
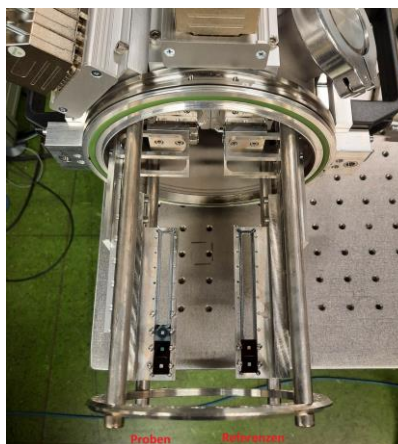
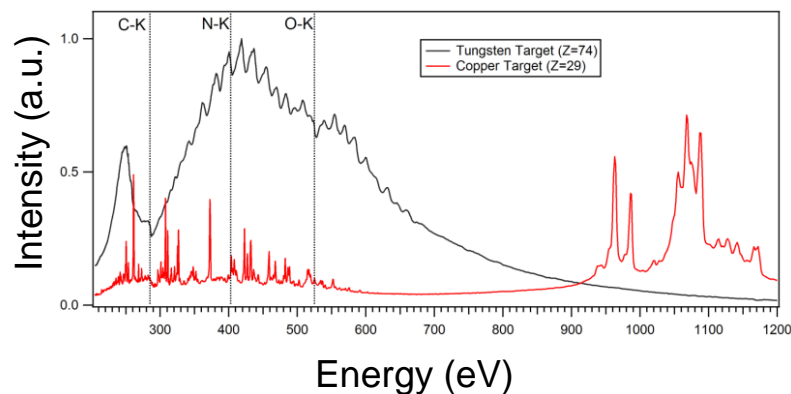
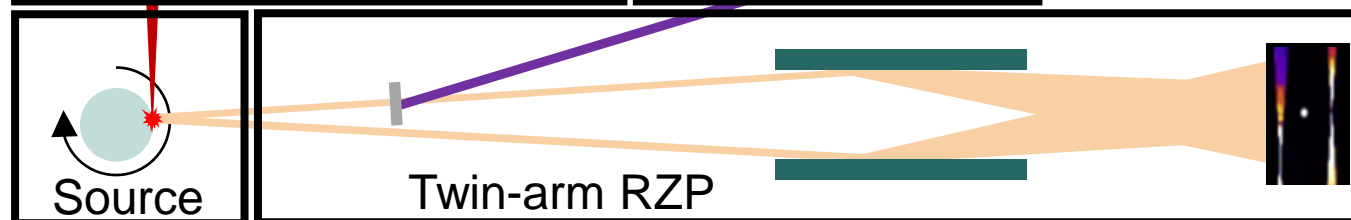


LPP SOURCE WITH 2 TWIN-ARM RZP SPECTROMETERS

Probe laser
190 mJ at 1064 nm pulse energy
100 Hz pulse repetition rate
 pulse duration of about **3 ns**



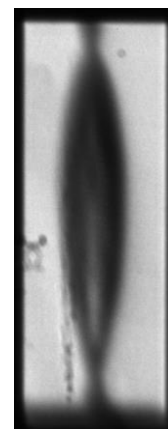
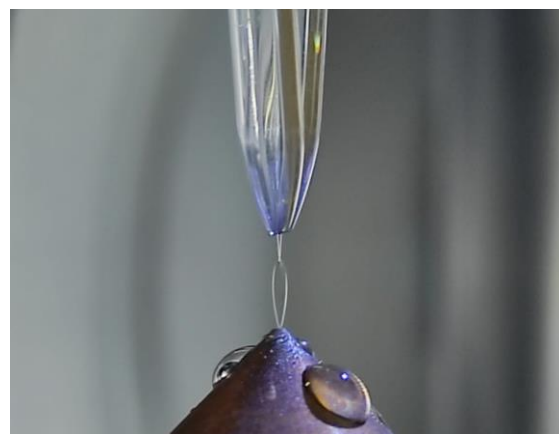
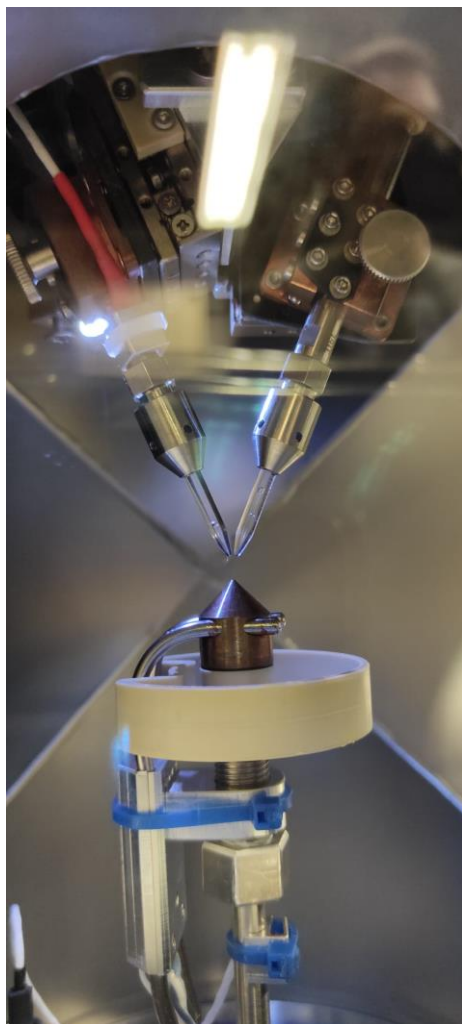
Pump laser
 no-gap wavelength tuning **192 - 2600 nm**
50 or 100 Hz pulse repetition rate
 up to **2 mJ** output pulse energy in UV
 less than **5 cm⁻¹** linewidth
about 3-4 ns pulse duration



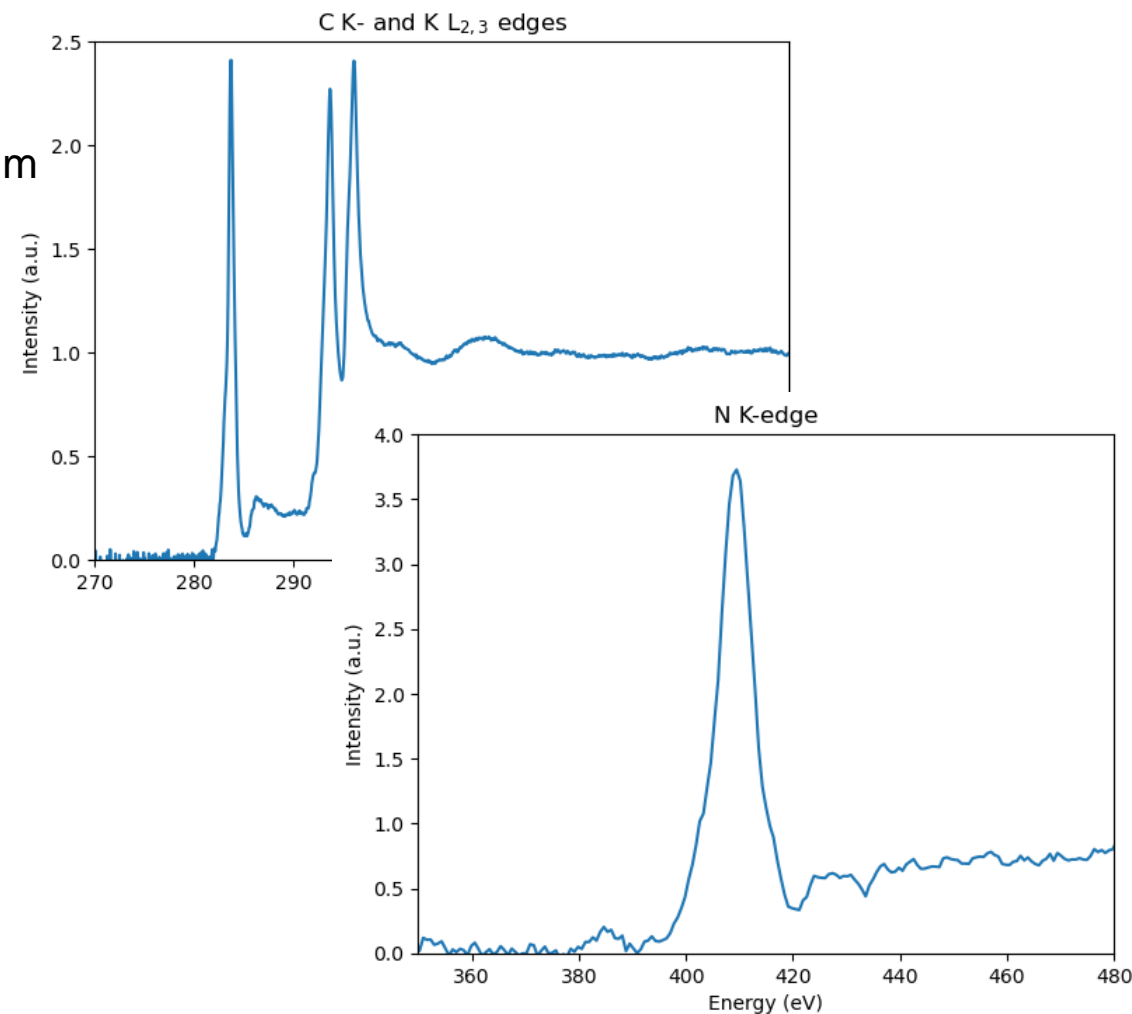
FLAT JET TO PROBE SAMPLES IN SOLUTION

Leafshaped liquid sheet with thicker rims and diminishing thickness of the median cross section (from top to bottom)

- Sheet thickness: 0,5 μm – 3 μm
- Area of minimal curvature: 100 μm x 100 μm to 500 μm x 500 μm (depending on jet size)
- Thickness stability: <1%
- Spatial stability <1 μm
- Temperature from -20° to +100° C

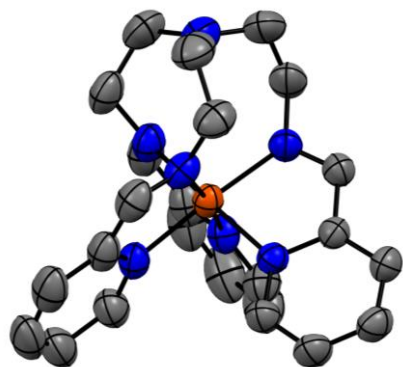


130 mMol $\text{K}_3[\text{Fe}(\text{CN})_6]$
20000 pulses for sample and for reference

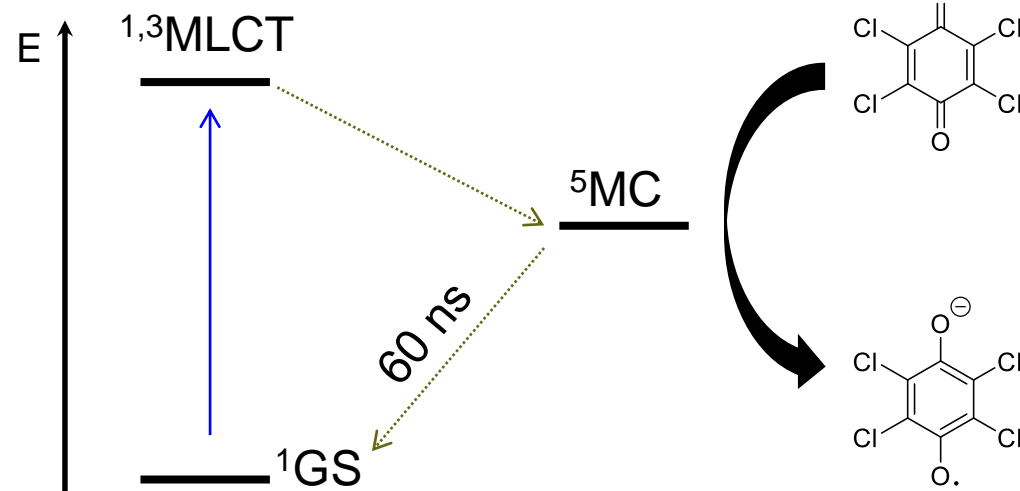


INVESTIGATION OF LONG-LIVED EXCITED STATES

Electron-Transfer Photochemistry of MC States



Inorganica Chim. Acta, **2004**, 357, 2390.



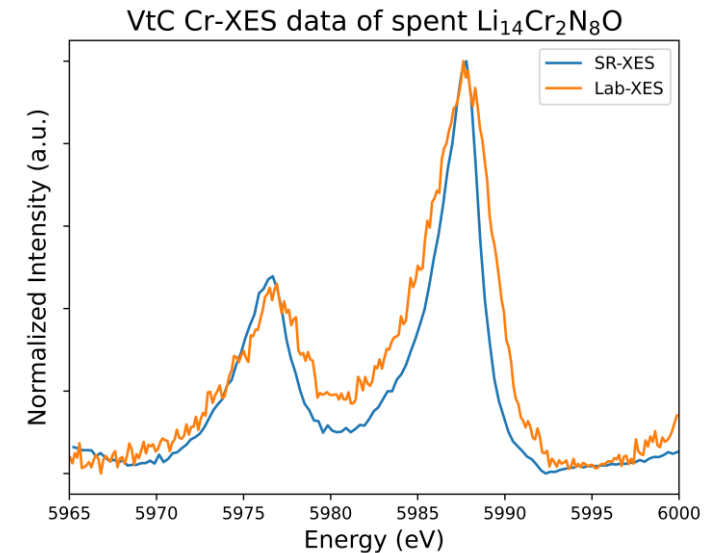
J. Am. Chem. Soc., **2000**, 122, 4092.
J. Am. Chem. Soc., **2020**, 142, 16229.

- Electron transfer from ^5MC state (localized in metal center)
- Investigation of transfer mechanism in a photoredox reaction

Courtesy of Issiah B. Lozada

OUTLOOK

- For XES: comparison of data collected across a range of elements between PINK beamline and in-house XES spectrometer
- Development of sample environments to accommodate different needs within the department on Inorganic Spectroscopy at the CEC
- Move towards time-resolved measurements in the soft X-ray energy range
- Commissioning of the new in-house XANES spectrometer with cross-comparison to the existing spectrometer



Thank you for your attention

Thanks to Serena DeBeer, John Carl Camayang, Christian Feike, Liqun Kang, Issiah Lozada, Philipp Manthey, Anna Scott, Vishwashri Srinivasan, Diana Tiburcio and the department of Inorganic Spectroscopy

Serena DeBeer acknowledges the ERC for funding of the in-house XES spectrometer

Acknowledgments to Birgit Kanngießner, Wolfgang Malzer, Christopher Schlesiger, Richard Gnewkow, and Daniel Grötzsch from the Technical University of Berlin and the Berlin Laboratory for Innovative X-ray spectroscopy